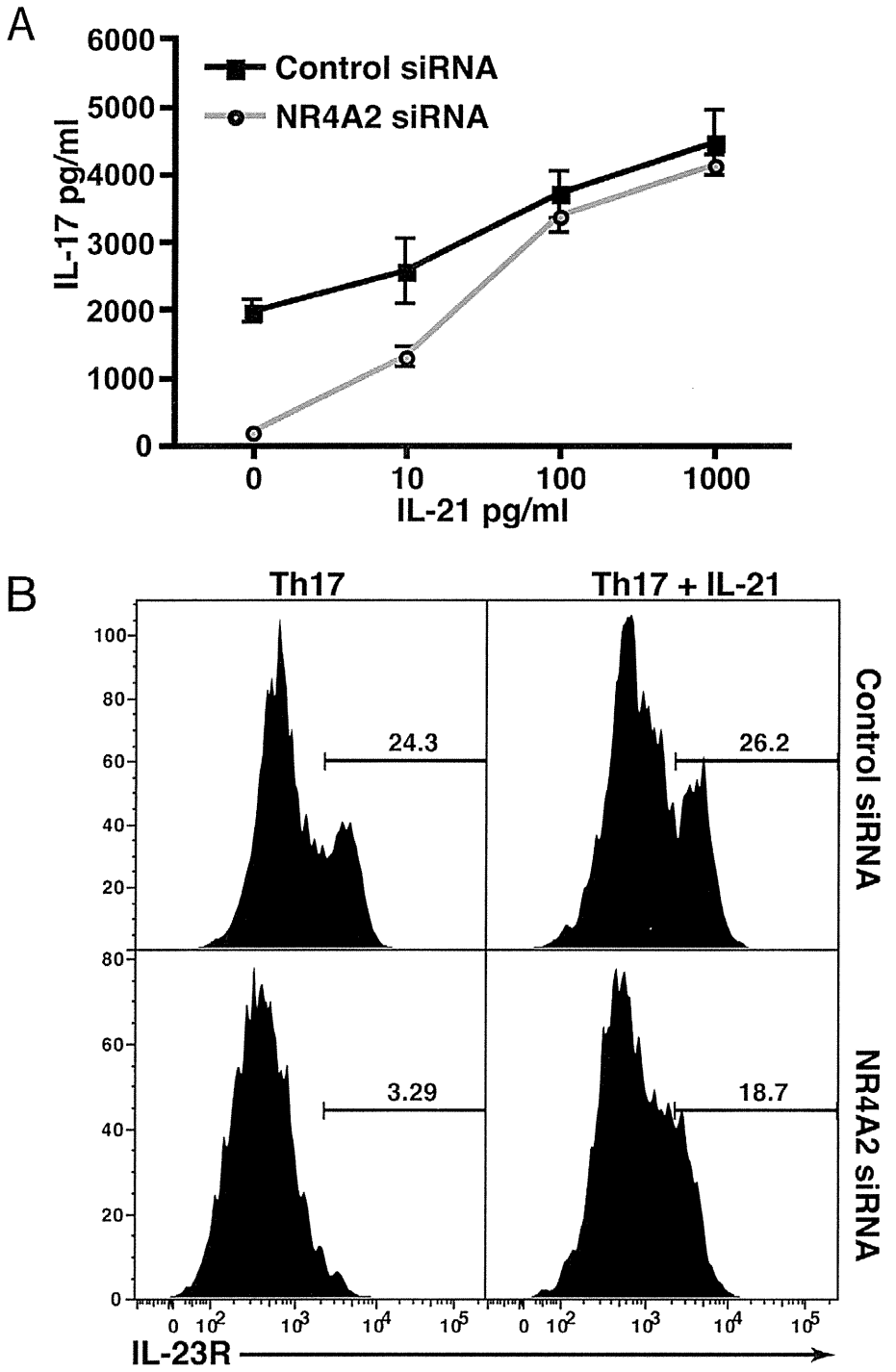

Figure 4. Exogenous IL-21 restores IL-17 production in the absence of NR4A2. Naïve $CD4^+$ T cells were transfected by electroporation with NR4A2-specific siRNA or scrambled control siRNA and were activated with 5 μg/ml plate-bound CD3-specific mAb and 0. 5 μg/ml soluble CD28-specific mAb in the presence of 20 ng/ml IL-6, 20 ng/ml IL-23, and 3 ng/ml TGF-β. To some wells, recombinant IL-21 was added as indicated. **A:** IL-17 was measured in the supernatants of control or NR4A2 siRNA-treated T cells by ELISA after 96 hours of culture under Th17 polarizing conditions in the presence or absence of IL-21 at the indicated concentrations. *$p<0.05$. Data are representative of 3 independent experiments. **B:** IL-23R expression was assessed by intracellular flow cytometric staining after 96 hours of culture under Th17 polarizing conditions in the presence (right plots) or absence (left plots) of 100 pg/ml recombinant IL-21 for control siRNA-treated T cells (top) and NR4A2 siRNA-treated T cells (bottom row). Data are representative of 2 independent experiments.
doi:10.1371/journal.pone.0056595.g004

later onset of EAE may reflect the reduced potency of the siRNA. We then tested the effect of injection of NR4A2 siRNA at a later timepoint. Interestingly, when the NR4A2 siRNA was given on day 10 post-EAE induction, clinical EAE was greatly reduced, and unlike treatment at day 0, no increase in disease was observed after day 20 (Fig. 5D). These results indicate that NR4A2 targeting

siRNA is not only preventative, but also therapeutic against the development of EAE. Furthermore, the CNS-infiltrating T cells also showed reduced expression of IL-21 and IL-23R (Fig. 5E&F), reminiscent of the *in vitro* blocking of NR4A2 during Th17 cell differentiation. Based on these data, we suggest that NR4A2 is a key factor for Th17 differentiation *in vivo* during the initiation of autoimmune responses via its control of IL-21 and IL-23R expression.

Discussion

In this study, we demonstrate that the orphan nuclear receptor NR4A2 is highly expressed by IL-17-secreting T cells infiltrating the target organ of EAE and EAU. When upregulation of NR4A2 was prevented *in vitro*, Th17-polarizing T cells expressing RORγt did not further differentiate into mature Th17 cell capable of producing IL-21 and IL-17. This inhibition of Th17 cell differentiation was associated with disruption of autocrine IL-21 signalling. *In vitro* analysis showed that adding exogenous IL-21 restored the ability of the NR4A2 knocked-down Th17 cells to express IL-23R and produce IL-17. Furthermore, *in vivo* injection of NR4A2 siRNA prevented the development of EAE by specifically inhibiting Th17 cell production of IL-17, but not affecting Th1 cells. Based on these findings, we propose that NR4A2 has direct effects on T cell pathogenicity or plays a critical role in continuous new Th17 differentiation and thus it orchestrates effector functions of Th17 cells in mediating autoimmune diseases.

Reagents that dampen the function of Th17 cells are of practical interest in clinical settings. Indeed, an IL-17A-specific antibody was efficacious in clinical trials of human psoriasis, uveitis, and rheumatoid arthritis [44]. Although the effects of IL-17 blockade on EAE appear to be only modest [45,46], clinical trials are currently in progress to test IL-17A-specific antibody treatment in MS patients. As Th17 cells probably generate a range of proinflammatory cytokines, it is debatable how effective a therapy targeting a single cytokine may prove. NR4A2 appears to control various molecules regulated by IL-21 signalling and therefore a drug targeting NR4A2 may prove more effective than an antibody against a single cytokine.

We previously described that forced expression of NR4A2 in resting T cells led to a modest increase in IFN-γ production following nonspecific stimulation and suggested that NR4A2 might be involved in both Th1 and Th17 cell responses [27]. In contrast, we here reveal that only Th17 cells were found to express NR4A2 in the lesions of EAE, implying that NR4A2 plays a more important role in Th17 cells than in Th1 cells during autoimmune inflammation. However, it is not surprising to see a reduced IFN-γ production in NR4A2 knocked-down T cells *in vitro* (Fig. 2A), since IL-21 has potentials to modulate IFN-γ production under particular conditions [47]. An unexpected report was that the absence of NR4A2 led to increased expression of IFN-γ [37]. The authors argued that the increased production of IFN-γ was due to reduced activity of $Foxp3^+$ regulatory T cells that are also dependent on NR4A2 [37]. However, this report does not contradict with our results, because in our *in vitro* experiments, we have explicitly removed regulatory T cells from the starting cell populations.

In agreement with previous studies [17,48], our results showed that autocrine IL-21 production would promote IL-23R expression and subsequent production of IL-17 during Th17 cell

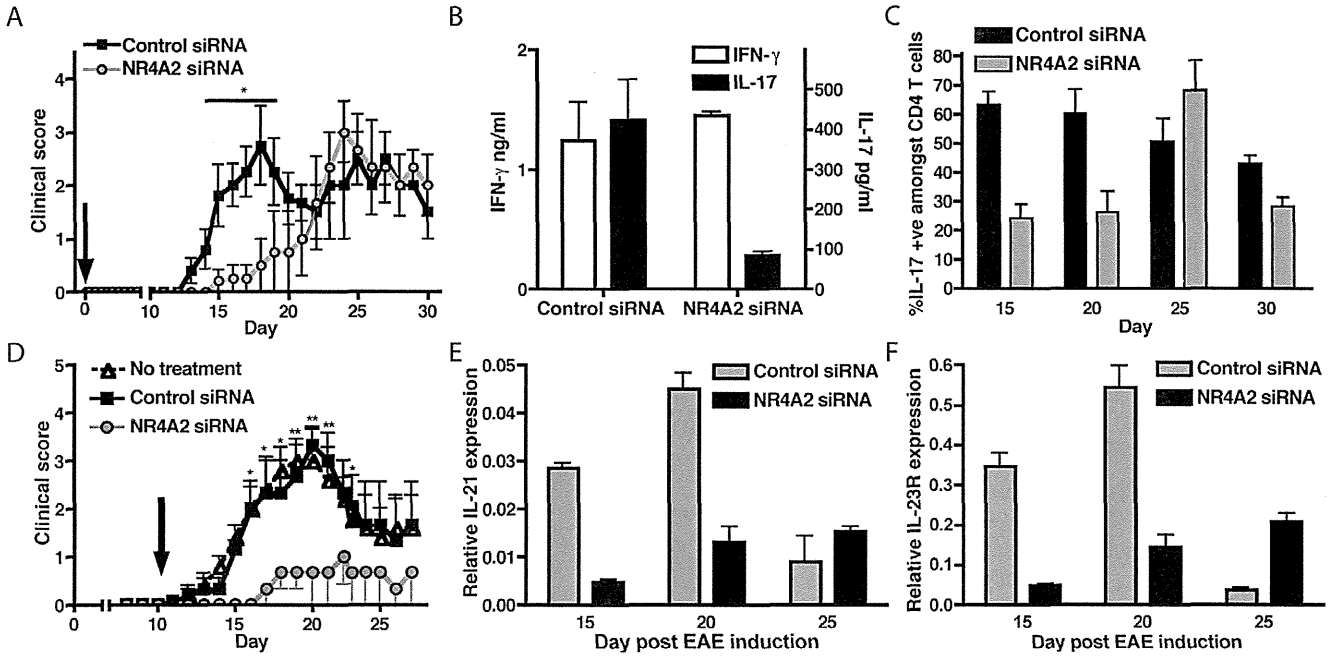

Figure 5. Systemic administration of NR4A2-specific siRNA reduces EAE severity. siRNA, either NR4A2-specific or control, was stabilized in a collagen matrix and administered *i.v.* to groups of C57BL/6 mice at the time of EAE induction. EAE was scored clinically (**A**) and at day 15 post-EAE induction, production of IL-17 and IFN-γ by CNS-infiltrating leukocytes restimulated with 20 μg/ml MOG peptide for 96 hours were assessed by ELISA (**B**). CNS-infiltrating T cells were also assessed for IL-17 production at a range of timepoints by intracellular flow cytometry (**C**). Data are representative of 3 independent experiments. Control or NR4A2-specific siRNA was applied to MOG-immunized mice at day 10 post-disease induction and disease was scored clinically (**D**). Timepoints correspond to a minimum of 5 animals and data are representative of 2 independent experiments. IL-21 and IL-23R expressions amongst CNS-infiltrating T cells were measured by real time PCR (**E&F**). Data are representative of 2 independent experiments. Clinical scores in panels A) and D) were tested with a two-way ANOVA test. *$p<0.01$, **$p<0.001$.
doi:10.1371/journal.pone.0056595.g005

differentiation. When NR4A2 upregulation was blocked by siRNA treatment, the production of IL-17 was greatly reduced, although RORγt expression was maintained, but exogenously added IL-21 restored IL-17 and IL-23R expression. Furthermore, NR4A2 also appeared to be required for the induction of the transcription factor that controls IL-21 secretion following Th17 differentiation, c-maf [41]. Moreover, lack of NR4A2 had little effect on RORγt expression, implying that this transcription factor is not associated with an IL-21-related pathway. It is interesting that IL-22 production is also maintained in the absence of NR4A2, despite the lack of IL-23R, suggesting that this cytokine could be produced via IL-23-independent pathways. TGF-β signals usually inhibit IL-22 production [16], however it is conceivable that these inhibitory signals are ineffective without NR4A2, thus allowing IL-22 secretion in the absence of increased IL-23R expression. Thus, NR4A2 modulation of Th17 cells may be limited to a role in the c-maf/IL-21 pathway, which ultimately controls IL-23R regulation and subsequent signalling. Given the critical role of IL-23 during pathogenic Th17 cell differentiation [16], the ability of NR4A2 siRNA to affect IL-23R expression by inhibiting IL-21 production cannot be ignored. It has been shown that IL-21 can drive Th17 differentiation [49] and thus enhance the initiation phase of EAE [50]. Therefore, the NR4A2-IL-21 pathway is particularly interesting as a therapeutic target. On the other hand, although a report claims that IL-21 is essential for Th17 differentiation [39], other reports showed Th17 differentiation in the absence of IL-21, albeit at a reduced level [14], and IL-17 production and EAE induction were not entirely blocked without IL-21 autocrine signals [51,52]. The discrepancy regarding the role of IL-21 in Th17 cell induction remains to be fully understood and it is possible that absence of IL-21 signalling in gene knockout mice may be compensated by an alternative cytokine signalling pathway. However, our data may be explained by direct effects of NR4A2 on IL-23R upregulation as well as on the c-maf/IL-21 pathway.

In conclusion, our findings highlight the application of siRNA *in vivo* to modulate immunologic pathways that generate pathogenic autoimmune responses. Furthermore, our discovery of the key role of NR4A2 signalling in Th17 differentiation and our identification of the involvement of NR4A2 in generating autoimmune response *in vivo* suggest a new target for intervention in Th17-mediated autoimmune disease. This view is supported by our direct demonstration that manipulation of NR4A2 expression by siRNA treatment in established disease ameliorated clinical symptoms. Thus, future therapies targeting NR4A2 may prove highly effective in treating particular autoimmune diseases.

Supporting Information

Figure S1 EAE or EAU was induced in C57BL/6 mice by immunization with MOG_{35-55} or $IRBP_{1-20}$ peptide in CFA. EAE was scored clinically (A). $CD4^+$ T cells were purified from the retina on the indicated days, and EAU disease severity was evaluated by flow cytometric enumeration of ocular infiltrates for EAU (B). Timepoints correspond to a minimum of 5 animals and data are representative of 3 independent experiments. A group of C57BL/6 mice received a low dose of STZ daily for 5 days. Clinical diabetes was tested by measurement of urine glucose level, with diabetes confirmed by consecutive urine glucose result of greater than ≥300 mg/dl (C). Plot C shows percentage diabetes. Other groups of C57BL/6 mice were immunized with peptides in CFA plus PTX either $OVA_{323-339}$ (OVA/CFA) or MOG_{35-55} (MOG/CFA). On day 22, splenocytes and leukocytes isolated from the relevant target organ (ND, OVA/CFA; CNS, EAE; pancreas, STZ) were restimulated with 20 mg/ml of the immunizing peptide, or with soluble anti-CD3 (for STZ); after 96 hours, IL-17 and IFN-γ were measured in supernatants by ELISA (D). NR4A2 expression by blood T cells was also measured at a range of timepoints (E). Timepoints correspond to a minimum of 5 animals and data are representative of 2 independent experiments.
(TIF)

Figure S2 Naïve $CD4^+$ T cells were transfected by electroporation with NR4A2-specific siRNA or scrambled control siRNA. Cells were then activated with 5 μg/ml plate-bound CD3-specific mAb and 0.5 μg/ml soluble CD28-specific mAb in the presence of 20 ng/ml IL-6, 20 ng/ml IL-23, and 3 ng/ml TGF-β. NR4A2 expression was assessed at a range of timepoints by RT PCR (A). Data are representative of 5 independent experiments. Cell proliferation of transfected cells following anti-CD3/anti-CD28 stimulation in the presence of Th1 (+10 ng/ml IL-12), Th17 (+20 ng/ml IL-6, 20 ng/ml IL-23, and 3 ng/ml TGF-β), or in the absence of polarizing cytokines was measured at 96 hours by the incorporation of ^{3}H-thymidine. Data are representative of 2 independent experiments.
(TIF)

Figure S3 Naïve $CD4^+$ T cells transfected by electroporation with NR4A2-specific siRNA or scrambled control siRNA were activated with plate-bound CD3-specific mAb and soluble CD28-specific mAb in the presence of 10 μg/ml IFN-γ-specific and IL-4-specific mAb, with either 20 ng/ml IL-6, 2 ng/ml TGF-β (IL-6+ TGF-β) or with 10 ng/ml TGF-β (TGF-β). Foxp3 expression at 96 hours as measured by real time PCR is shown in plot A. Data shown represent averages of 4 independent experiments. Naïve $CD4^+$ T cells were transfected by electroporation with 2 siRNAs: either Foxp3-specific siRNA or relevant scrambled control siRNA and with either NR4A2-specific siRNA or relevant scrambled control siRNA. This yielded 4 cell types: 1) Foxp3 control/NR4A2 control (C/C); 2) Foxp3 control/NR4A2 siRNA (C/N); 3) Foxp3 siRNA/NR4A2 control (F/C); and 4) Foxp3 siRNA/NR4A2 siRNA (F/N). Cells were then activated with plate-bound CD3-specific mAb and soluble CD28-specific mAb in the presence of 10 μg/ml IFN-γ-specific and IL-4-specific mAb with either 20 ng/ml IL-6, 2 ng/ml TGF-β (IL-6+ TGF-β) or with 10 ng/ml TGF-β (TGF-β). Plot B shows IL-17 production from each of 4 siRNA-treated cell types at 96 hours as measured by ELISA. Data are representative of 2 independent experiments. siRNA, either NR4A2-specific or control, was stabilized in a collagen matrix and administered *i.v.* to groups of C57BL/6 mice at the time of EAE induction. At the indicated timepoints, CNS-infiltrating T cells were FACS-sorted and NR4A2 expression was assessed by RT PCR (A). CNS-infiltrating leukocytes from day 15 post-EAE induction from control or NR4A2 siRNA-treated mice were restimulated with PMA/ionomycin for 5 hours, and IL-17 and IFN-γ production were visualized by intracellular flow cytometric staining (B). Data are representative of 3 independent experiments
(TIF)

Figure S4 siRNA, either NR4A2-specific or control, was stabilized in a collagen matrix and administered *i.v.* to groups of C57BL/6 mice at the time of EAE induction. At the indicated timepoints, CNS-infiltrating T cells were FACS-sorted and NR4A2 expression was assessed by RT PCR (A). CNS-infiltrating leukocytes from day 15 post-EAE induction from control or NR4A2 siRNA-treated mice were restimulated with PMA/ionomycin for 5 hours, and IL-17 and IFN-γ production

were visualized by intracellular flow cytometric staining (B). Data are representative of 3 independent experiments.
(TIF)

Author Contributions

Conceived and designed the experiments: BR SO TY. Performed the experiments: BR. Analyzed the data: BR SO. Wrote the paper: BR SO TY.

References

1. Sospedra M, Martin R (2005) Immunology of multiple sclerosis. Annu Rev Immunol 23: 683–747.
2. Bettelli E, Korn T, Kuchroo VK (2007) Th17: the third member of the effector T cell trilogy. Curr Opin Immunol 19: 652–657.
3. Damsker JM, Hansen AM, Caspi RR (2010) Th1 and Th17 cells: adversaries and collaborators. Ann N Y Acad Sci 1183: 211–221.
4. Korn T, Oukka M, Kuchroo V, Bettelli E (2007) Th17 cells: effector T cells with inflammatory properties. Semin Immunol 19: 362–371.
5. Goverman J (2009) Autoimmune T cell responses in the central nervous system. Nat Rev Immunol 9: 393–407.
6. Jager A, Dardalhon V, Sobel RA, Bettelli E, Kuchroo VK (2009) Th1, Th17, and Th9 effector cells induce experimental autoimmune encephalomyelitis with different pathological phenotypes. J Immunol 183: 7169–7177.
7. Luger D, Silver PB, Tang J, Cua D, Chen Z, et al. (2008) Either a Th17 or a Th1 effector response can drive autoimmunity: conditions of disease induction affect dominant effector category. J Exp Med 205: 799–810.
8. Steinman L (2008) A rush to judgment on Th17. J Exp Med 205: 1517–1522.
9. Man S, Ubogu EE, Ransohoff RM (2007) Inflammatory cell migration into the central nervous system: a few new twists on an old tale. Brain Pathol 17: 243–250.
10. Matusevicius D, Kivisakk P, He B, Kostulas N, Ozenci V, et al. (1999) Interleukin-17 mRNA expression in blood and CSF mononuclear cells is augmented in multiple sclerosis. Mult Scler 5: 101–104.
11. Hirota K, Duarte JH, Veldhoen M, Hornsby E, Li Y, et al. (2011) Fate mapping of IL-17-producing T cells in inflammatory responses. Nat Immunol 12: 255–263.
12. Bettelli E, Carrier Y, Gao W, Korn T, Strom TB, et al. (2006) Reciprocal developmental pathways for the generation of pathogenic effector TH17 and regulatory T cells. Nature 441: 235–238.
13. Korn T, Bettelli E, Oukka M, Kuchroo VK (2009) IL-17 and Th17 Cells. Annu Rev Immunol 27: 485–517.
14. Korn T, Bettelli E, Gao W, Awasthi A, Jager A, et al. (2007) IL-21 initiates an alternative pathway to induce proinflammatory T(H)17 cells. Nature 448: 484–487.
15. Das J, Ren G, Zhang L, Roberts AI, Zhao X, et al. (2009) Transforming growth factor beta is dispensable for the molecular orchestration of Th17 cell differentiation. J Exp Med 206: 2407–2416.
16. Ghoreschi K, Laurence A, Yang XP, Tato CM, McGeachy MJ, et al. (2011) Generation of pathogenic T(H)17 cells in the absence of TGF-beta signalling. Nature 467: 967–971.
17. Cua DJ, Sherlock J, Chen Y, Murphy CA, Joyce B, et al. (2003) Interleukin-23 rather than interleukin-12 is the critical cytokine for autoimmune inflammation of the brain. Nature 421: 744–748.
18. McGeachy MJ, Cua DJ (2007) The link between IL-23 and Th17 cell-mediated immune pathologies. Semin Immunol 19: 372–376.
19. Law SW, Conneely OM, DeMayo FJ, O'Malley BW (1992) Identification of a new brain-specific transcription factor, NURR1. Mol Endocrinol 6: 2129–2135.
20. Perlmann T, Wallen-Mackenzie A (2004) Nurr1, an orphan nuclear receptor with essential functions in developing dopamine cells. Cell Tissue Res 318: 45–52.
21. Le WD, Xu P, Jankovic J, Jiang H, Appel SH, et al. (2003) Mutations in NR4A2 associated with familial Parkinson disease. Nat Genet 33: 85–89.
22. Pearen MA, Muscat GE (2010) Minireview: Nuclear Hormone Receptor 4A Signaling: Implications for Metabolic Disease. Mol Endocrinol 24: 1–13.
23. Aherne CM, McMorrow J, Kane D, FitzGerald O, Mix KS, et al. (2009) Identification of NR4A2 as a transcriptional activator of IL-8 expression in human inflammatory arthritis. Mol Immunol 46: 3345–3357.
24. O'Kane M, Markham T, McEvoy AN, Fearon U, Veale DJ, et al. (2008) Increased expression of the orphan nuclear receptor NURR1 in psoriasis and modulation following TNF-alpha inhibition. J Invest Dermatol 128: 300–310.
25. Saijo K, Winner B, Carson CT, Collier JG, Boyer L, et al. (2009) A Nurr1/CoREST pathway in microglia and astrocytes protects dopaminergic neurons from inflammation-induced death. Cell 137: 47–59.
26. Satoh J, Nakanishi M, Koike F, Miyake S, Yamamoto T, et al. (2005) Microarray analysis identifies an aberrant expression of apoptosis and DNA damage-regulatory genes in multiple sclerosis. Neurobiol Dis 18: 537–550.
27. Doi Y, Oki S, Ozawa T, Hohjoh H, Miyake S, et al. (2008) Orphan nuclear receptor NR4A2 expressed in T cells from multiple sclerosis mediates production of inflammatory cytokines. Proc Natl Acad Sci U S A 105: 8381–8386.
28. Klemann C, Raveney BJ, Klemann AK, Ozawa T, von Horsten S, et al. (2009) Synthetic retinoid AM80 inhibits Th17 cells and ameliorates experimental autoimmune encephalomyelitis. Am J Pathol 174: 2234–2245.
29. Raveney BJ, Copland DA, Nicholson LB, Dick AD (2008) Fingolimod (FTY720) as an acute rescue therapy for intraocular inflammatory disease. Arch Ophthalmol 126: 1390–1395.
30. Copland DA, Wertheim MS, Armitage WJ, Nicholson LB, Raveney BJ, et al. (2008) The clinical time-course of experimental autoimmune uveoretinitis using topical endoscopic fundal imaging with histologic and cellular infiltrate correlation. Invest Ophthalmol Vis Sci 49: 5458–5465.
31. Mensah-Brown EP, Shahin A, Al-Shamisi M, Wei X, Lukic ML (2006) IL-23 leads to diabetes induction after subdiabetogenic treatment with multiple low doses of streptozotocin. Eur J Immunol 36: 216–223.
32. Fraser JM, Janicki CN, Raveney BJ, Morgan DJ (2006) Abortive activation precedes functional deletion of CD8+ T cells following encounter with self-antigens expressed by resting B cells in vivo. Immunology 119: 126–133.
33. Raveney BJ, Copland DA, Dick AD, Nicholson LB (2009) TNFR1-dependent regulation of myeloid cell function in experimental autoimmune uveoretinitis. J Immunol 183: 2321–2329.
34. Shao H, Liao T, Ke Y, Shi H, Kaplan HJ, et al. (2006) Severe chronic experimental autoimmune uveitis (EAU) of the C57BL/6 mouse induced by adoptive transfer of IRBP1–20-specific T cells. Exp Eye Res 82: 323–331.
35. Elias D, Prigozin H, Polak N, Rapoport M, Lohse AW, et al. (1994) Autoimmune diabetes induced by the beta-cell toxin STZ. Immunity to the 60-kDa heat shock protein and to insulin. Diabetes 43: 992–998.
36. Zhou L, Lopes JE, Chong MM, Ivanov, II, Min R, et al. (2008) TGF-beta-induced Foxp3 inhibits T(H)17 cell differentiation by antagonizing RORgammat function. Nature 453: 236–240.
37. Sekiya T, Kashiwagi I, Inoue N, Morita R, Hori S, et al. (2011) The nuclear orphan receptor Nr4a2 induces Foxp3 and regulates differentiation of CD4+ T cells. Nat Commun 2: 269.
38. Zhou L, Ivanov, II, Spolski R, Min R, Shenderov K, et al. (2007) IL-6 programs T(H)-17 cell differentiation by promoting sequential engagement of the IL-21 and IL-23 pathways. Nat Immunol 8: 967–974.
39. Nurieva R, Yang XO, Martinez G, Zhang Y, Panopoulos AD, et al. (2007) Essential autocrine regulation by IL-21 in the generation of inflammatory T cells. Nature 448: 480–483.
40. Ivanov, II, Zhou L, Littman DR (2007) Transcriptional regulation of Th17 cell differentiation. Semin Immunol 19: 409–417.
41. Bauquet AT, Jin H, Paterson AM, Mitsdoerffer M, Ho IC, et al. (2009) The costimulatory molecule ICOS regulates the expression of c-Maf and IL-21 in the development of follicular T helper cells and TH-17 cells. Nat Immunol 10: 167–175.
42. Veldhoen M, Hirota K, Westendorf AM, Buer J, Dumoutier L, et al. (2008) The aryl hydrocarbon receptor links TH17-cell-mediated autoimmunity to environmental toxins. Nature 453: 106–109.
43. Takeshita F, Minakuchi Y, Nagahara S, Honma K, Sasaki H, et al. (2005) Efficient delivery of small interfering RNA to bone-metastatic tumors by using atelocollagen in vivo. Proc Natl Acad Sci U S A 102: 12177–12182.
44. Hueber W, Patel DD, Dryja T, Wright AM, Koroleva I, et al. (2011) Effects of AIN457, a fully human antibody to interleukin-17A, on psoriasis, rheumatoid arthritis, and uveitis. Sci Transl Med 2: 52ra72.
45. Hofstetter HH, Ibrahim SM, Koczan D, Kruse N, Weishaupt A, et al. (2005) Therapeutic efficacy of IL-17 neutralization in murine experimental autoimmune encephalomyelitis. Cell Immunol 237: 123–130.
46. Komiyama Y, Nakae S, Matsuki T, Nambu A, Ishigame H, et al. (2006) IL-17 plays an important role in the development of experimental autoimmune encephalomyelitis. J Immunol 177: 566–573.
47. Monteleone G, Monteleone I, Fina D, Vavassori P, Del Vecchio Blanco G, et al. (2005) Interleukin-21 enhances T-helper cell type I signaling and interferon-gamma production in Crohn's disease. Gastroenterology 128: 687–694.
48. Langrish CL, Chen Y, Blumenschein WM, Mattson J, Basham B, et al. (2005) IL-23 drives a pathogenic T cell population that induces autoimmune inflammation. J Exp Med 201: 233–240.
49. Leonard WJ, Spolski R (2005) Interleukin-21: a modulator of lymphoid proliferation, apoptosis and differentiation. Nat Rev Immunol 5: 688–698.
50. Vollmer TL, Liu R, Price M, Rhodes S, La Cava A, et al. (2005) Differential effects of IL-21 during initiation and progression of autoimmunity against neuroantigen. J Immunol 174: 2696–2701.
51. Coquet JM, Chakravarti S, Smyth MJ, Godfrey DI (2008) Cutting edge: IL-21 is not essential for Th17 differentiation or experimental autoimmune encephalomyelitis. J Immunol 180: 7097–7101.
52. Sonderegger I, Kisielow J, Meier R, King C, Kopf M (2008) IL-21 and IL-21R are not required for development of Th17 cells and autoimmunity in vivo. Eur J Immunol 38: 1833–1838.

A Trifluoromethyl Analogue of Celecoxib Exerts Beneficial Effects in Neuroinflammation

Alessandra Di Penta[1,2☯], Asako Chiba[3,4☯], Iraide Alloza[1,2,5], Ane Wyssenbach[6], Takashi Yamamura[3], Pablo Villoslada[7], Sachiko Miyake[3,4], Koen Vandenbroeck[1,2,5*]

1 Neurogenomiks Laboratory, University of Basque Country (UPV/ EHU), Zamudio, Spain, **2** Achucarro Basque Center for Neuroscience, Zamudio, Spain, **3** Department of Immunology, National Institute of Neuroscience, National Center of Neurology and Psychiatry, Tokyo, Japan, **4** Department of Immunology, Juntendo University School of Medicine, Tokyo, Japan, **5** IKERBASQUE, Basque Foundation for Science, Bilbao, Spain, **6** Neurotek Laboratory, University of Basque Country (UPV/EHU), Zamudio, Spain, **7** Center of Neuroimmunology, Institute of Biomedical Research August Pi Sunyer (IDIBAPS) – Hospital Clinic of Barcelona, Barcelona, Spain

Abstract

Celecoxib is a selective cyclooxygenase-2 (COX2) inhibitor. We have previously shown that celecoxib inhibits experimental autoimmune encephalomyelitis (EAE) in COX-2-deficient mice, suggestive for a mode of action involving COX2-independent pathways. In the present study, we tested the effect of a trifluoromethyl analogue of celecoxib (TFM-C) with 205-fold lower COX-2 inhibitory activity in two models of neuroinflammation, i.e. cerebellar organotypic cultures challenged with LPS and the EAE mouse model for multiple sclerosis. TFM-C inhibited secretion of IL-1β, IL-12 and IL-17, enhanced that of TNF-α and RANTES, reduced neuronal axonal damage and protected from oxidative stress in the organotypic model. TFM-C blocked TNF-α release in microglial cells through a process involving intracellular retention, but induced TNF-α secretion in primary astrocyte cultures. Finally, we demonstrate that TFM-C and celecoxib ameliorated EAE with equal potency. This coincided with reduced secretion of IL-17 and IFN-γ by MOG-reactive T-cells and of IL-23 and inflammatory cytokines by bone marrow-derived dendritic cells. Our study reveals that non-coxib analogues of celecoxib may have translational value in the treatment of neuro-inflammatory conditions.

Citation: Di Penta A, Chiba A, Alloza I, Wyssenbach A, Yamamura T, et al. (2013) A Trifluoromethyl Analogue of Celecoxib Exerts Beneficial Effects in Neuroinflammation. PLoS ONE 8(12): e83119. doi:10.1371/journal.pone.0083119

Editor: Giovambattista Pani, Catholic University Medical School, Italy

Received June 14, 2013; **Accepted** October 31, 2013; **Published** December 11, 2013

Funding: This study was supported by Grant Grupos de Investigación (UPV/EHU; ref. IT512-10) to KV; Ministerio de Ciencia e Inovación (MICINN, Madrid, Spain; ref. SAF2008-00433 and SAF2012-32118) and by the Gobierno Vasco's SAIOTEK Program (ref. 'ERtek' S-PE09UN33) to KV; Instituto de Salud Carlos III: FIS PI041445 (MIOTRED) to PV; Juan de la Cierva program of the Ministerio de Ciencia y Innovacion (MICINN, ref. JCI-2009-04462) to AdP. The funders had no role in study design, data collection and analysis, decision to publish, or preparation of the manuscript.

Competing interests: The authors declare that Pablo Villoslada, as one of the co-authors of the manuscript, is a PLOS ONE Editorial Board. This does not alter the authors' adherence to all the PLOS ONE policies on sharing data and materials.

* E-mail: k.vandenbroeck@ikerbasque.org

☯ These authors contributed equally to this work.

Introduction

Nonsteroidal anti-inflammatory drugs are indicated for the treatment of a variety of chronic inflammatory diseases and act by inhibiting prostaglandin H synthase (also known as cyclooxygenase, COX). Two forms of this enzyme are known: COX1 that is expressed constitutively in most tissues and plays a role in the protection of the gastrointestinal mucosa, renal hemodynamics, and platelet thrombogenesis, and COX2 that is inducible and expressed in cells involved in inflammation [1]. Selective COX2 inhibitors (i.e., celecoxib, rofecoxib, and valdecoxib) have been developed for the treatment of inflammatory diseases [2] minimizing gastrointestinal adverse reactions caused by COX-1 inhibition.

Celecoxib has been demonstrated to act via both COX2-dependent and -independent pathways, both associated with potent anti-tumour effects [3,4]. Recently, we have shown that both celecoxib and its trifluoromethyl analogue, TFM-C (4-[5-(4-trifluoromethylphenyl)-3-(trifluoromethyl)- 1*H*-pyrazol-1-yl]benzenesulfonamide) that displays 205-fold lower COX2-inhibitory activity, can inhibit secretion of (hetero)dimeric cytokines belonging to the interleukin-12 (IL-12) family (including IL-23 and p40 homodimers) with similar IC_{50}'s. Using recombinant cell lines, TFM-C caused Ca^{2+}-dependent chaperone-mediated cytokine subunit retention in the endoplasmic reticulum (ER) coupled to degradation via the ER stress protein HERP [5,6]. This observation provided a translational extension of recent findings in our lab of functional chaperone interaction peptide motifs conserved in cytokines as

well as of multiple ATP-dependent cytokine-chaperone interactions during ER transit of cytokines [7-9]. Perturbance of ER Ca^{2+} by celecoxib and non-coxib analogues triggers a cellular response known as "unfolded protein response" (UPR) [4,10,11]. The UPR has a dual role in the cell survival: in normal conditions works as a pro-survival response mediated by the blockage of protein translation and activation of transcription factors that can restore the ER function to its normal physiological state. However, if ER stress persists, its pro-survival function can switch to a pro-apoptotic program, finally leading to cell death [12,13].

COX-2 inhibitors such as indomethacin or rofecoxib exert beneficial effects in EAE; the latter, for example, by modulating Th1/Th2 responses [14,15]. Recently, we have shown that celecoxib inhibits EAE [16]. In particular, we found that celecoxib in contrast to other COX-2 inhibitors such as nimesulid, prevented EAE by inhibiting the infiltration of inflammatory cells into the central nervous system, MOG-specific Th1 cytokine production and expression of adhesion molecules and MCP-1 [16]. This protective effect was not mediated via COX2 inhibition since it was also observed in COX2-deficient mice [16]. We have demonstrated that celecoxib and its analogue TFM-C exerted beneficial effects in two models of arthritis: collagen-induced arthritis (CIA) and collagen antibody-induced arthritis (CAIA). In particular, TFM-C, more so than celecoxib, inhibited the severity of CIA and CAIA by suppressing the activation of mast cells and the production of inflammatory cytokines by macrophages [17]. Nevertheless, celecoxib and other COX2 inhibitors display adverse effects that may compromise further implementation in clinical practice. Increased risk for myocardial infarction and stroke in drug recipients have been reported [18-22]. Comparison of cardiovascular risks profiles of celecoxib vs the non-selective nonsteroidal anti-inflammatory drug naproxen and ibuprofen is currently addressed in the PRECISION trial (http://clinicaltrials.gov/show/NCT00346216). Suppression of prostacyclin (PGI2) and prostaglandin E2, two COX-2-derived products, may provide protective constraint mechanisms on processes such as thrombogenesis and atherogenesis [23]. In rodents, celecoxib predisposes to platelet activation and arterial thrombosis by suppressing PGI2 [24]. Similarly, selective inhibition of COX-2 can enhance platelet–vessel wall interactions and platelet adhesion *in vivo* increasing the risk of thrombosis [25].

We hypothesized that TFM-C may constitute a new drug candidate that retains the beneficial effects of celecoxib in the EAE model while its much decreased COX2 inhibitory activity would render it less adverse in terms of cardiovascular risk. In this study, we have analyzed the effect of TFM-C on cytokine secretion, demyelination, and axonal damage in mice cerebellar organotypic cultures, a model of neuroinflammation, and assessed its activity in the EAE model.

Materials and Methods

Ethics statement

Animals were handled in accordance with the European Communities Council Directive (Directive 2010/63/EU), the Spanish regulations for the procurement and care of experimental animals (RD 53/2013, February 1st), and the study was approved by the Ethical Committee on Animal Research of the University of Basque Country (UPV/EHU). EAE experiments were approved by the Institutional Animal Care and Use Committee of the National Institute of Neuroscience (Tokyo, Japan).

Table 1. List of primary antibodies used for immunofluorescence (IF) and western blot (WB) studies.

Antigen	Description	Dilution	Company
ARMET	ARMET antibody, Rabbit	1:2000 (WB)	AbCam
HERP	Homocysteine-induced endoplasmic reticulum protein, Mouse	1:200/1:400 (IF) 1:2000 (WB)	Hirabayashi Y [6].
Iba1	Ionized calcium binding adaptor molecule 1: anti-Iba 1, Rabbit	1:400/1:500 (IF)	Wako
iNOS	Inducible nitric oxide synthase: purified rabbit anti-iNOS/NOS type II	1:200 (IF) 1:500 (WB)	BD Bioscience
LC3B	LC3B (D11) XP™ Rabbit mAb	1:1000 (WB)	Cell Signaling
MBP	Myelin Basic Protein; Rat anti-MBP (82-87) antibody	1:200 (IF)	Serotec
NFH	Neurofilament heavy (phosphorylated and non-phosphorylated NfH): rabbit polyclonal antiserum against the 200 kD Neurofilament Heavy	1:200 (IF)	AbCam
NFL	Neurofilament light C28E10, Rabbit mAb	1:200 (IF)	Cell Signaling
PARK2	Rabbit polyclonal to Parkin	1:750 (WB)	AbCam
RAB24	Purified Mouse Anti-Rab24	1:1000 (WB)	BD Bioscience
SMI32	non-phosphorylated neurofilament heavy SMI32, Mouse	1:200 (IF)	Stenberg
TNF-α	Anti-Murine TNF-alpha, Rabbit	1:300 (IF)	MBL
Tubulin	α-Tubulin Antibody [HRP], mAb, Mouse	1:2000	GenScript

doi: 10.1371/journal.pone.0083119.t001

Materials and animals

All animal experiments in this study were performed using C57BL/6J mice (Harlan Laboratories, Italy). C57BL/6J Jcl mice used in EAE experiments were purchased from CLEA Japan, Inc. Mice were maintained in a temperature-controlled environment with food and water *ad libitum* at 12-hour light/12-hour dark cycle. The animals used in this study were 8 weeks old for EAE experiments and 8 days old for cerebellar organotypic cultures experiments. TFM-C was synthesized by Onyx Scientific (Sunderland, UK). All antibodies used in this work are indicated in Table 1.

Induction and clinical assessment of EAE

C57BL/6J Jcl (B6) female mice (n = 5-6 per group, 7-8 weeks old) were immunized subcutaneously at the base of the tail with 100 μg of myelin oligodendrocyte glycoprotein 35-55

(MOG35-55) peptide (amino acid sequence, MEVGWYRSPFSRVVHYRNGK, derived from mouse MOG) dissolved in 0.1 ml phosphate buffered saline (PBS) and 0.1 ml CFA containing 1 mg of Mycobacterium tuberculosis strain H37Ra (*Mtb* H37Ra). Shortly after immunization and 48 h later, the mice were injected i.p. with 200 ng of Bordetella pertussis toxin (List Biological Laboratories). Mice were randomly assigned to three treatment groups receiving intraperitoneal injections of TFM-C or celecoxib at doses of 10 µg/g, or control vehicle every other day from the day of immunization. In the control group, the sample size is n=5-6 per group (16 animals in total) and in the TFM-C-treated group n=4-5 animals per group (14 animals in total). The experiment was repeated three times in order to respect the directives for reduction of the number of animals in animal experiments. Only 5 animals were used in the celecoxib-treated group because we have assessed the effect of celecoxib in a previous study [16]. Clinical scores of EAE were assigned daily as follows: 0 = normal; 1 = weakness of the tail and/or paralysis of the distal half of the tail; 2 = loss of tail tonicity; 3 = partial hind limb paralysis; 4 = complete hind limb paralysis; 5= forelimb paralysis or moribund; 6 = death. The EAE scoring was conducted by personnel unaware of treatment-group assignments. Mice were sacrificed with lethal dose of diethyl ether.

Cerebellar organotypic cultures

The cerebellar slice culture was based on published protocols [26,27]. Organotypic slice cultures were prepared from 8-day old C57BL/6 mice. Cerebella were cut at 350 µm with a McIlwain Tissue Chopper (The Mickle Laboratory Engineering Co. LTD.) and three slices were plated on Millicell-CM culture inserts. From 10 mice we obtained approximately 90 slices. Cultures were incubated at 37°C and 5% CO_2 in 50 % basal medium with Earle's salt, 25% Hank's buffered salt solution, 25% inactivated horse serum, 5mg/ml glucose, 0,25mM L-glutamine and 25µg/ml Pen/Strep (Invitrogen). Cerebellar slices were maintained in culture for 7 days and then pre-treated with 50 µM of TFM-C for 2 hours followed by stimulation with 15 µg/ml of lipopolysaccharide (LPS; Sigma L4391) for 6 and 24 hours, or as indicated.

BV2 cell line

BV2 cells were provided by Prof. Carlos Matute (University of the Basque Country, Leioa, Spain) [28] and were maintained in Dulbecco's Modified Eagle's medium (DMEM) containing 5% heat inactivated Fetal Bovine Serum (FBS), 4 mM L-Glutamine (SAFC biosciences), 20 mM Hepes (Sigma) and 25µg/ml Pen/Strep (Invitrogen) antibiotics at 37°C in a humidified chamber with 5% $C0_2$. Before treatment, cells were washed twice with DMEM, then pre-incubated with TFM-C (30 µM or 50 µM) for 2 hours and stimulated with 1 µg/ml LPS (Sigma L4391) for 3, 6, 12 and 24 hours.

HEK-293 cell line and PCR arrays

Human embryonic kidney-293 cells (HEK-293; Invitrogen), were cultured in DMEM (Sigma) supplemented with 10 % fetal bovine serum (Sigma), 2 mM L-glutamine (Invitrogen) and 25µg/ml Pen/Strep (Invitrogen). Cells were washed twice with DMEM and incubated with TFM-C (50 µM) for 3, 6, 12 and 24 hours. RNA was extracted and reverse transcribed using RT^2 First Strand Kits (SABiosciences, address), followed by profiling of the expression of 84 key genes each belonging to UPR, Ubiquitination and Autophagy Pathway RT^2 Profiler PCR Arrays (SABiosciences, address). Data was analyzed using the manufacturer's PCR Array Data Analysis Software.

Total protein extraction and Western Blot

Three cerebellar slices, HEK-293 and BV2 cells were homogenised by stroke dounce homogenization in 60 µl of ice-cold RIPA buffer (150mM NaCl; 50mM Tris-Cl, pH 7.5; 1% NP-40; 0.5% DOC; 0.1% SDS) and the lysate was centrifuged at 15.000 x g for 10 min at 4°C. Total protein concentration was estimated by the Bradford assay (Bio-Rad). 10 µg of total protein from cerebellar slices, BV2 or HEK-293 cells were separated by SDS-PAGE on Bio-Rad TGX Stain-Free precast gels. The gels were exposed to UV irradiation for 5 min and then total protein was transferred onto a nitrocellulose membrane (Bio-Rab). UV irradiation activates a covalent reaction between the trihalocompound and tryptophan residues on the proteins in the gel, resulting in UV induced fluorescence (Figure S5). Total protein was visualized with ChemiDoc (Bio-Rad) and quantified using Image Lab 4.0 software. The filters were pre-wetted in blocking buffer (5% dried non-fat milk or 2% casein, 20 mM Tris pH 8, 300 mM NaCl, 0.1% Tween-20) and then hybridized for 2h or O.N. with primary antibodies in blocking buffer (Table 1); the secondary antibodies (HRP-conjugated anti-mouse or anti-rabbit from Cell Signaling) were used at a dilution of 1:2000.

RNA isolation and Quantitative RT-PCR (QPCR)

Cerebellar organotypic cultures, HEK-293 and BV2 cells were lysed with TRI reagent (Sigma). Chloroform was added for phase separation with RNA remaining in the aqueous phase. RNA was precipitated with 2-propanol and the pellet resuspended in DNA/RNA free water (Invitrogen). RNA was quantified using Nanodrop 2000c spectrophotometer (Thermo Scientific). 200 ng of mice organotypic cultures, HEK-293 and BV2 cells RNA were reverse-transcribed to cDNA using random primers according to manufacturer's protocol (Applied biosystems). QPCR was performed with the Supermix for SsoFast EvaGreen (Biorad) on a 7500 Fast Real-Time PCR System (Applied Biosystems). For each target gene, QPCR QuantiTect Primer Assay were used (Qiagen). Expression levels for the transcripts of interest were normalized to that of endogenous glyceraldehyde 3-phosphate dehydrogenase or hypoxanthine phosphoribosyltransferase 1 (Hprt1). The data were calculated as percentage fold expression or $2^{-\Delta\Delta Ct}$ relative to the average of the untreated control group, unless indicated otherwise.

Quansys Q-Plex™ Array Chemiluminescent and ELISA

For Q-Plex system analysis, 30 µl of medium from mice cerebellar organotypic cultures treated with LPS or LPS/TFM-C were used. Mouse Cytokine Stripwells (16-plex) were used following the manufacturer's instructions (Quansys Bioscience).

The chemiluminescent signal was acquired with Bio-Rad ChemiDoc camera and the image was analyzed with Q-View Software (Quansys Bioscience). BV2 cells were pre-treated with TFM-C (30 μM or 50 μM) for 2 hours and then stimulated with LPS for different periods of time (0, 3, 6, 12 and 24 hours) and the culture supernatants were collected to quantify the secreted IL-1β, tumor necrosis factor (TNF-α) and IL-6. Mouse ELISA Kits were used according to the manufacturer's instructions (eBioscience, BD Bioscience, R&D Systems).

Immunofluorescence microscopy

Cerebellar slices were fixed with 4% paraformaldehyde (PFA) for 40 min, washed with PBS for 10 min, and blocked at RT for 2 hours in 10% normal goat serum (NGS; Vector Laboratories) and 0.5% Triton X-100 in PBS. The slices were incubated overnight at 4°C with the distinct primary antibodies (Table 1) in blocking solution (10% NGS and 0.3% Triton X-100 in PBS). The slices were washed and incubated in blocking solution containing the secondary antibody mixture and washed three times with 0.1% Triton X-100 in PBS. BV2 cells were fixed with 4% PFA for 20 min, washed with PBS for 10 min, permeabilized for 20 min with 0.2% Triton X-100 in PBS and blocked at RT for 30 min in 10% FBS (Invitrogen) in PBS. The cells were incubated 1 hour with the Iba1 and HERP (1:400; kindly supplied by Dr. Yasuhiko Hirabasyashi, Tohuku University, Japan) or TNF-α primary antibodies in blocking solution (10% FBS in PBS). After washing, the cells were incubated in blocking solution containing the secondary antibody mixture, washed three times with PBS and incubated with DAPI (1:50000; Molecular Probes) in PBS. The secondary antibodies used were mouse IgG Cy2-linked, rabbit IgG Cy3-linked (from goat, 1:200; GE Healthcare) and goat anti-rat IgG Alexa Fluor 488 (1:200; Molecular Probes). The slices and coverslips were mounted in Gel/Mount anti-fading mounting medium (Biomeda) and pictures were captured by confocal scanning microscopy (Olympus Fluoview FV500) from single images all through the whole tissue or cells (but avoiding the surface of the culture in contact with air).

DAPI and Propidium iodite (PI) staining

12 hours before LPS/TFM-C (3, 6, 12 and 24 hours) treatment BV2 cells were incubated over night with PI (250 ng/ml; Fluka) and then fixed with 4% PFA. The cells were washed three times with PBS and then incubated with DAPI (1:50000; Molecular Probes) in PBS. Coverslips were embedded in Fuoro-Gel (Electron Microscopy Science). Images were recorded using the confocal microscope and analyzed using the ImageJ program (version 1.40).

Flow cytometry of BV2 cells

The expression of intracellular TNF-α was evaluated by cytofluorometry. $1x10^6$ cells were plated and after 24 hours treated with LPS (1μg/ml) or pre-treated with TFM-C for 2 hour and then stimulated with LPS/TFM-C for 3, 6, and 24 hours. The cells were detached with trypsin, washed in PBS, pelleted at 300 g for 10 min and fixed with PFA 2% for 20 min. Then, cells were permeabilized with 0,2% Triton in PBS for 20 min, blocked with 10% NGS in PBS for half hour, and incubated with primary antibody TNF-α (1:100; MBL) for 1 hour in blocking solution. After washing, cells were incubated with secondary antibody (1:500 goat anti-mouse AlexaFluo 488; LifeTechnology) in blocking solution for 30 min in darkness. Following further washes, cells were pelleted and the fluorescence was analyzed using a Gallios cytometer (Beckman Coulter) at excitation/emission wavelengths of 488/515-535 nm.

Astrocyte-enriched cell culture

Primary cultures of cerebral cortical astrocytes were prepared as described previously by McCarthy and de Vellis (1980) [29]. Briefly, forebrains were removed from the skulls, the meninges were carefully excised under a dissecting microscope, and the cortices were isolated. Tissue was incubated for 15 min in Hank's Balanced Salt Solution (HBSS) with tripsine and DNAase, the reaction was stopped with DMEM supplemented with 10% FBS and centrifuged to remove cellular debris. Cells were resuspended in Iscove's Modified Dulbecco's Medium supplemented with 10% FBS and antibiotic/antimycotic solution, and the cells were dissociated by passage through needles of decreasing diameter (21 G and 23 G) 10 times. Cells were re-centrifuged and then resuspended in Iscove's Modified Dulbecco's Medium supplemented with 10% FBS and antibiotic/antimycotic solution. Cells were seeded into poly-D-lysine-coated flasks, and maintained in culture at 37°C and 5% CO_2. The culture medium was renewed the day after seeding, and twice a week thereafter. After 8 days, cultures were shaken (3 hours, 350 rpm) to deplete microglial cells and were trypsinized and plated onto poly-D-lysine-coated, 24-well plates.

Statistical analysis

All experiments were performed at least three times, and control cultures were time-matched with testing cultures. The values were expressed as the means ± SEM. ANOVA or Student's t-tests were used to determine statistical significance, as indicated, and all analyses were performed using SPSS 15.0 software (IBM). EAE clinical or pathological scores for the group of mice are presented as the mean group clinical score +SEM, and statistical differences were analyzed with a non-parametric Mann-Whitney U-test.

Results

TFM-C modulates cytokine release and suppresses oxidative stress and axonal damage in mouse celerebellar organotypic cultures

The effect of TFM-C on cytokine release was assessed in a model of neuroinflammation consisting of mice cerebellar organotypic cultures stimulated with LPS, by means of a multiplex ELISA-based Q-Plex assay system (see Materials and Methods). Of 16 assessed cytokines, 5 were identified of which LPS-induced secretion was modulated by TFM-C (Figure 1A). While LPS challenge induced varying levels of the pro-inflammatory cytokines IL-1α, IL-1β, IL-3, IL-5, IL-6, IL-10, IL-12, IL-17, MCP-1, IFN-γ, TNF-α, MIP-1α and RANTES

(Figure 1A), TFM-C treatment significantly decreased IL-1β, IL-12 and IL-17 release and increased TNF-α and RANTES. mRNA levels of a subset of these cytokines were also measured in mice organotypic cultures treated with LPS or LPS/TFM-C. HERP was included as a marker for ER stress that is inducible by TFM-C [6,9]. TFM-C treatment decreased IL-1β mRNA expression levels at 6 and 24 hours, but those of IL-6 and IL-10 only at 24 hours (Figure 1B). In contrast, TNF-α mRNA levels were significantly higher after 6 hours of TFM-C treatment and this trend persisted at the 24 h time-point (non-significant). This mirrored the increased levels of secreted TNF-α demonstrated in Figure 1A. No significant changes were observed for IL-12p35, IL-23p19 and HERP mRNAs.

Next we scored the effect of TFM-C on LPS-induced oxidative stress, demyelination and axonal damage in the organotypic model [30-33] using immunofluorescence, immunoblot and QPCR. The analyzed markers included iNOS for oxidative stress, CNPase for demyelination, SMI32 for axonal damage, and HERP for ER stress. Immunofluorescence showed that TFM-C increased HERP protein expression in microglia identified with Iba1, and upregulated HERP protein in the total culture (Figure 2A, panel a; Figure 2B). Axonal damage was visualized by dual immunostaining for both total (phosphorylated and non-phosphorylated) NFH and non-phosphorylated NFH (SMI32; Figure 2A, panel d). In response to LPS, non-phosphorylated NFH was found to accumulate at 3.5 higher levels compared to total NFH, suggestive for induction of axonal dysfunction. Furthermore, LPS-induced axonal damage was visible via formation of swollen structures (beading and spheroids; white box in Figure 2A, panel d) associated with impaired axonal transport and transection [34]. TFM-C prevented formation of swollen structures and maintained LPS-induced non-phosphorylated neurofilament levels to those of baseline control (Figure 2D). In contrast, TFM-C treatment had no effect on demyelination assessed by MBP/NFL immunofluorescence (Figure 2A, panel c) or CNPase expression (Figure 2B). Finally, pretreatment with TFM-C prior to LPS challenge strongly reduced iNOS expression determined by immunofluorescence, Western Blot and QPCR (Figure 2A, panel b; Figure 2B & C). TFM-C did not affect expression of MHCII (Figure S1). Taken together, these results indicate that TFM-C partially counteracted LPS-induced effects reminiscent of an anti-inflammatory, anti-oxidant and neuroprotective mode of action.

TFM-C suppresses cytokine release and induces UPR / ER stress in BV2 microglia cells

Previously, we have demonstrated that TFM-C inhibits secretion of the (hetero)dimeric IL-12 family cytokines IL-12, $p40_2$ and IL-23 through a Ca^{2+}-dependent mechanism involving chaperone-mediated cytokine retention in the ER coupled to degradation via HERP protein, and that TFM-C dramatically upregulates *HERP* gene expression in various cell lines [5,6,9]. In organotypic cultures, virtually no effect was seen on mRNA production of *HERP* at 6 and 12 hours of LPS/TFM-C treatment in compared with LPS stimulation (Figure 1B). To verify whether TFM-C is capable of inducing ER stress in microglia, the mouse microglial BV2 cell line was used. Specifically, we measured mRNA of HERP and IL-23p19, both of which are induced by ER stress [5,6,35]. BV2 cells were pre-treated with TFM-C (30 and 50 μM) for 2 hours and then stimulated with LPS for 3, 6, 12 and 24 hours in the presence or absence of TFM-C, which showed significant dose-dependent up-regulation of IL-23p19 and HERP (Figure 3B). Figure 3C shows that co-treatment of LPS with TFM-C led to increased accumulation of HERP in microglial cells (Figure 3C, panel a). In immunoblot, HERP protein levels were increased in BV2 cells at 12 hours of treatment in the presence of 50 μM of TFM-C plus LPS compared to LPS-only challenge (Figure 3C, panels b and c; Figure S5). To answer the question whether TFM-C is also able to block cytokine release from BV2 cells, IL-1β, IL-6 and TNF-α mRNA and secreted protein levels were analyzed (Figure 3A). TFM-C significantly decreased LPS-induced IL-1β mRNA and protein secretion starting at 6 hours of treatment. However, TFM-C exerted biphasic opposing effects on TNF-α mRNA levels at 3 (decrease) versus 24 (increase) hours compared to LPS-only challenge; of note, TFM-C suppressed secreted TNF-α protein levels throughout the duration of the experiment. For IL-6, no significant changes were observed in mRNA levels while the secreted protein was down-regulated at 12 hours of TFM-C treatment. To rule out occurrence of apoptotic cell death as contributing factor in suppression of cytokine secretion, cells were stained with DAPI and PI which is only incorporated by cells that have suffered membrane damage. TFM-C/LPS treatment decreased cell viability with approximately 4%, similar to LPS-only treated cells (Figure 3D). To identify additional UPR/ER stress-regulated genes potentially involved in altered cytokine folding/assembly/secretion, the effect of TFM-C on transcription of 252 genes belonging to UPR, autophagy and ubiquitination pathways was analyzed in HEK-293 cells (Figure S2A). We identified 36 genes with a fold increase > 2.5 and confirmed *HERP* as the gene showing the fifth highest degree of upregulation by TFM-C (fold increase of 9.1 in the UPR PCR Arrays). *DDIT3* (CHOP), a primordial ER stress response gene [13,36], was identified with some distance as the gene showing the highest degree of induction by TFM-C (36-fold). Further analysis of the kinetics of upregulation by TFM-C of 5 of these genes, *PARK2, ARMET, FBXO4, RAB24* and *MAP1LC3B*, in addition to *HERP*, was performed in both HEK-293 and BV2 cells (Figure S2B and S2C). At the protein level, only HERP, MAP1LC3B and ARMET showed clear changes in the kinetics of their production in HEK-293 cells. In BV2 cells, TFM-C significantly decreased PARK2 expression at 3 and 12 hours, and increased RAB24 expression at 3 hours both compared with LPS-treated cells. No modification in MAP1LC3B and ARMET protein expression was observed (Figure S2D). Thus, TFM-C induces a gene expression signature predominantly enriched for UPR/ER stress response and ubiquitination pathway genes, including to a lesser extent also some genes involved in autophagy (Figure S2A). Pending mechanistic studies, this suggests that its suppressive effect on cytokine secretion may be functionally related to alterations in protein transit and turnover pathways, as suggested in our previous work [5,6,9,17].

A a

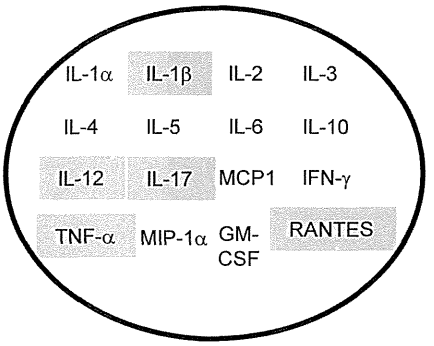

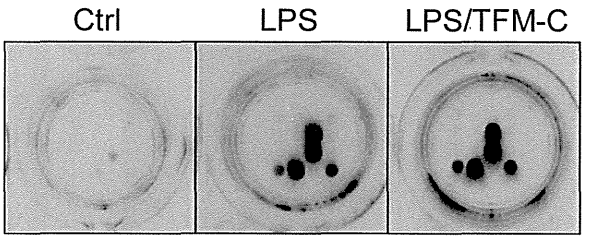

b

Cytokine	Ctrl pg/ml ±sd	LPS pg/ml (±sd)	LPS/TFM-C pg/ml (±sd)	% increase or decrease
IL-1α	9,7±5,4	31,8 (±13,5)	34,6)±17,2)	+8,1
IL-1β	70,7±37,4	299,9 (±26,2)	234,3 (±20,4)*	-21,9
IL-2	ND	ND	ND	ND
IL-3	ND	31,5 (±6,4)	16,2 (±11,8)	-48,6
IL-4	8,3±10,4	18,1 (±3,7)	10,5 (±7,6)	-42,3
IL-5	2,0±4,9	331,2 (±56,4)	431,4 (±58,7)	+30,2
IL-6	ND	4125,2 (±270,8)	4144,0 (±140,2)	+0,5
IL-10	ND	25,9 (±1,9)	25,1 (±3,7)	-3,1
IL-12p70	5,6±5,9	73,4 (±21,8)	33,6 (±8,9)*	-54,6
IL-17	ND	102,5 (±26,9)	54,7 (±9,9)*	-46,6
MCP-1	ND	2237,3 (±124,0)	2240,9 (±104,8)	+0,3
IFN-γ	12,3±19,5	91,8 (±20,5)	70,0 (±20,0)	-23,8
TNF-α	2,0±2,4	229,4 (±35,2)	436,6 (±27,1)*	+90,3
MIP-1α	ND	6354,5 (±351,2)	6243,2 (±283,9)	-1,7
GMCSF	ND	ND	ND	ND
RANTES	6,3±4,6	3649,3 (±182,2)	11340,0 (±2800,1)*	+210,7

B

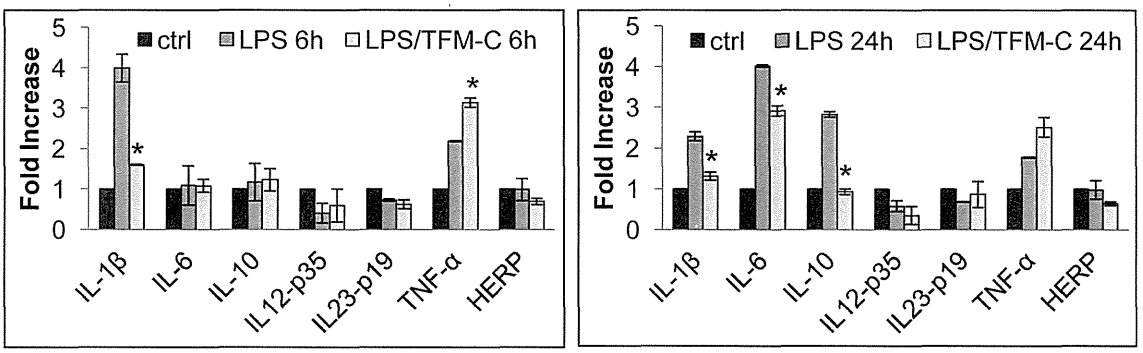

Figure 1. Effect of TFM-C on cytokine production in organotypic cerebellar cultures. A) After 7 *DIV* organotypic cultures were treated with TFM-C (50μM) for 6h and then stimulated with 15μg/ml LPS for 24h in presence of TFM-C. Panel a) Lay-out of cytokine-specific antibody spots in the 16-plex cytokine Stripwell array (left image) and visualization of cytokine-specific chemiluminescence in culture medium of LPS-treated organotypic cultures in the absence or presence of TFM-C (right images). Cyotkine levels significantly affected by TFM-C are highlighted in grey. Panel b) pg/ml of cytokines were indicated. sd: standard deviation. ND: not determinable. B) Effect of TFM-C on IL-1β, IL-6, IL-10, IL-12p35, IL-23p19, TNF-α and HERP mRNA in organotypic cultures stimulated by LPS for 6h and 24h in presence or absence of 50μM TFM-C. The levels of mRNA are shown as *n*-fold increase compared with baseline level (-) and normalized to those of the housekeeping gene *Hprt1*. Asterisks indicate significant differences at *<*P* 0.05 compared with LPS control by ANOVA test.

doi: 10.1371/journal.pone.0083119.g001

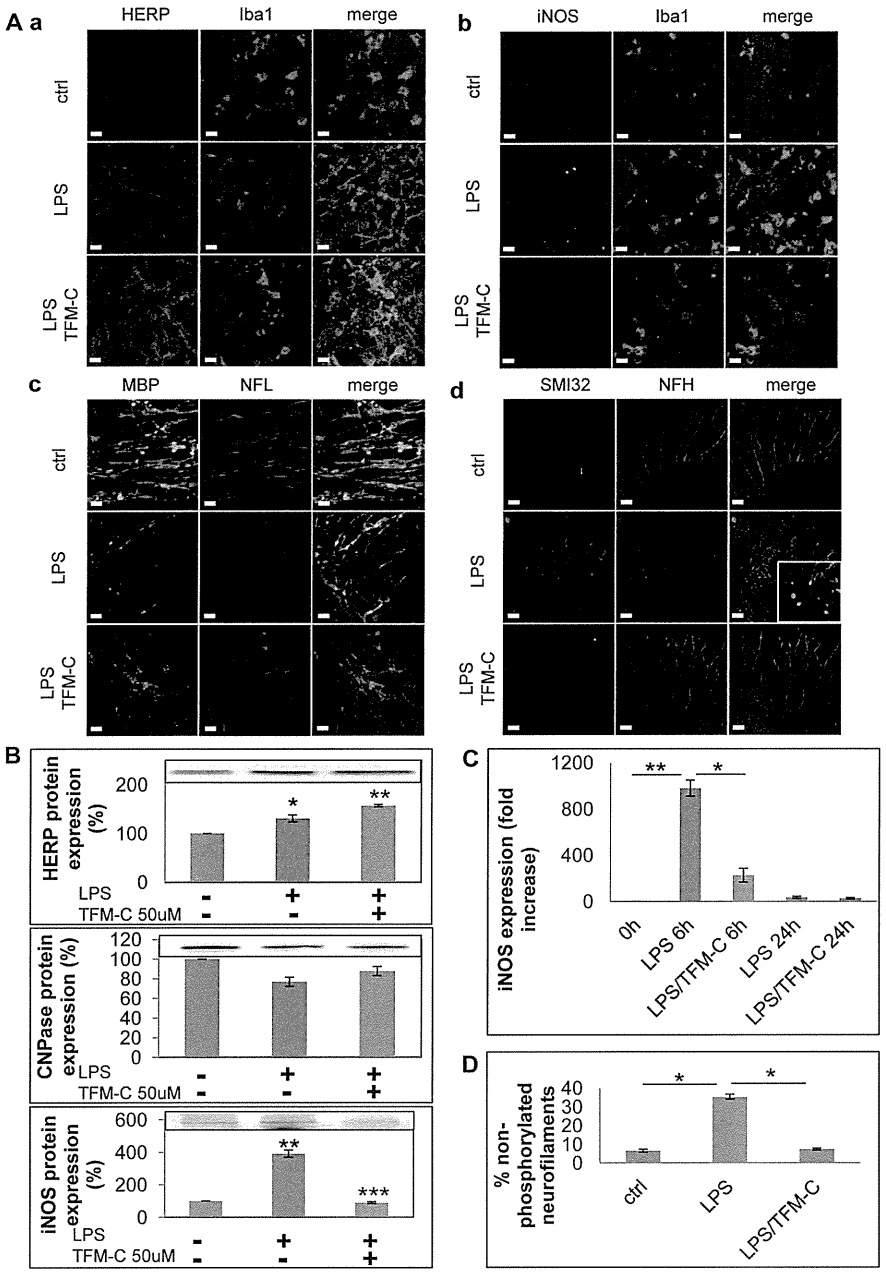

Figure 2. Effect of TFM-C on ER stress, oxidative stress, demyelination and axonal damage in organotypic cerebellar cultures. A) Organotypic cultures were stimulated with LPS for 24h or pre-treated with TFM-C (50μM) for 2h and then stimulated with LPS/TFM-C for 24h. Panel a-b: immunostaining for Iba1 (red) and HERP or iNOS (green). Panel c: immunostaining for NFL (red) and MBP (green); Panel d: immunistaining for total neurofilament-heavy (NFH; red) and non-phosphorylated neurofilament (SMI32; green). In the white box inset are shown axonal spheroids and occurrence of axonal transection (end-bulbs). Scale bar 10μm. B) 10μg of total protein were loaded for HERP, CNPase and iNOS Western blot analysis. Quantification of band intensity was calculated in the graphs below after normalization for total protein loaded. Results are expressed as percentage compared to the LPS only (100%). Error bars indicate the standard error. **P*<0.05, ***P*<0.001, ****P*<0.001 by ANOVA test. C) After 7 *DIV* organotypic cultures were treated with TFM-C for 2h and then stimulated with 15μg/ml LPS for 6 and 24h. iNOS mRNA expression was analyzed by quantitative PCR. The levels of mRNA are shown as *n*-fold increase compared with the level of baseline condition (-) and normalized to those of the housekeeping gene *Hprt1*. All values represent the averages of three independent experiments. Error bars indicate the standard error. **P*<0.05, ***P*<0.01, ****P*<0.001 by ANOVA test. D) Percentage of non-phosphorylated neurofilaments with respect to total neurofilaments in cerebellar cultures stimulated for 24h with LPS in presence or absence of TFM-C. Error bars indicate the standard error. **P* <0.05 by ANOVA test.

doi: 10.1371/journal.pone.0083119.g002

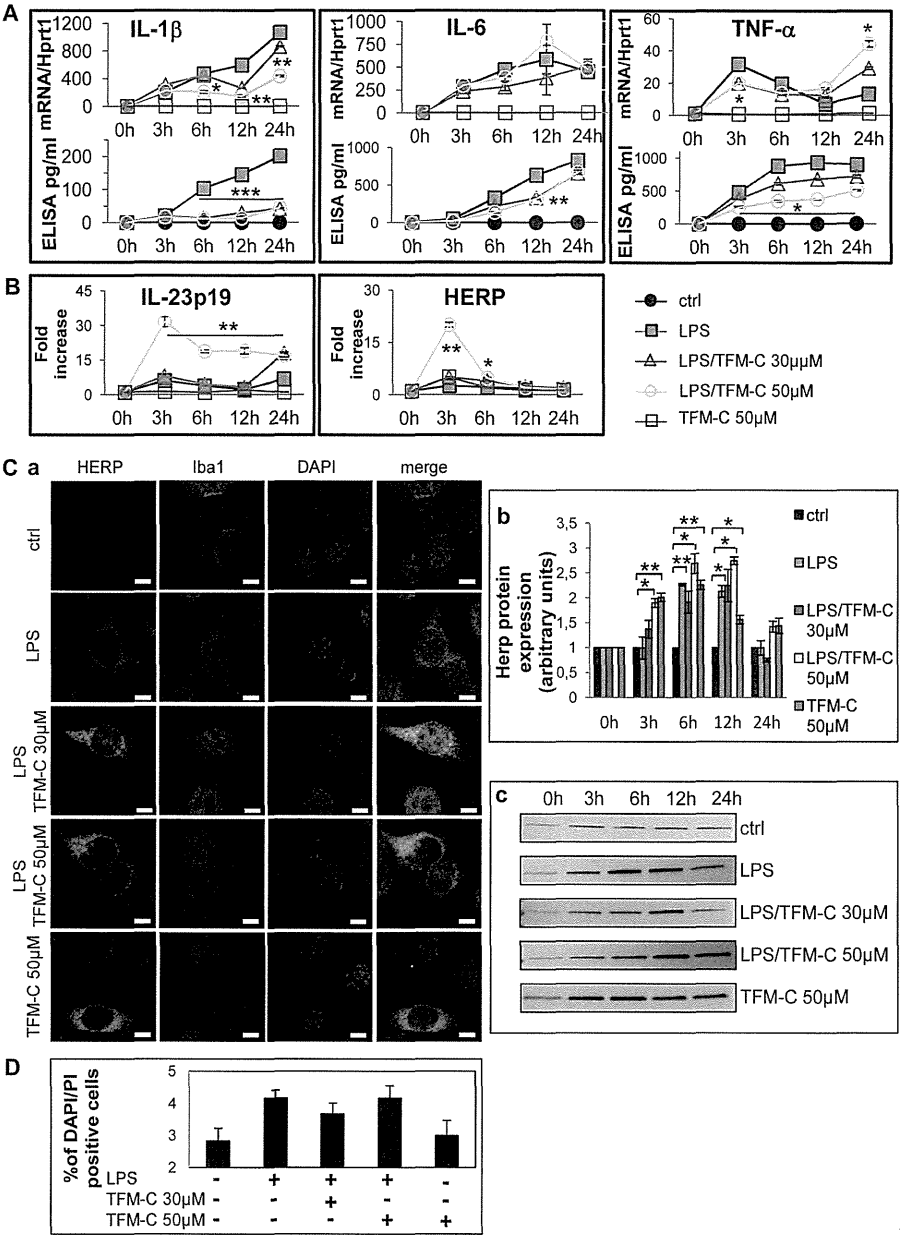

Figure 3. Effect of TFM-C on HERP and cytokine mRNA and protein production in BV-2 cells. BV2 cells were treated with TFM-C (30 or 50μM) for 2h and then stimulated with LPS (1μg/ml) for different times in presence or absence of TFM-C. A) Quantification of the kinetics of mRNA production and cytokine secretion (IL-1β, IL-6 and TNF-α). All values represent the averages of three independent experiments. Lower graphs represent cytokine-specific mRNA quantified by QPCR, while the upper graphs represents amount of secreted cytokine quantified using specific ELISA kits. Asterisks indicate significant differences at $*P< 0.05$, $**P<0.01$, $***P<0.001$ between TFM-C-treated and LPS-treated cells at each time point using ANOVA test. B) Effect of TFM-C (30 and 50μM) on IL-23p19 and HERP mRNAs in BV2 cells stimulated with LPS. The levels of mRNA levels are shown as fold increase. Asterisks indicate significant differences at $*P < 0.05$ and $**P<0.01$ compared with LPS only using ANOVA test. C) Effect of TFM-C on HERP protein expression. BV2 cells were treated with TFM-C (50μM) or pretreated with TFM-C for 2h (30 and 50μM) and then stimulated with LPS in presence of TFM-C. Panel a) Immunofluorescence for HERP (green), Iba1 (red) and DAPI (blue) at 12h of LPS/TFM-C or TFM-C treatment. Scale bar 5μm. Panel b-c) 10μg of total protein were loaded for HERP Western blot analysis. Results were expressed as arbitrary units respect to the control at same time point. Error bars indicate the standard error. $*P<0.05$ by ANOVA test. D) Effect of TFM-C treatment (50μM) on the viability of BV2 cells. Apoptotic cells were measured by double propidium iodite (PI) and DAPI staining, and the percentage of damaged DNA and condensed chromatin was calculated at 24h of LPS/TFM-C treatment.

doi: 10.1371/journal.pone.0083119.g003

TFM-C induces intracellular retention of TNF-α in BV2 microglia but increases its secretion from primary astrocytes

As demonstrated in Figure 3A, TFM-C reduces secreted levels of IL-1β and TNF-α from BV2 microglial cells. To clarify whether TNF-α was retained intracellularly, an immunofluorescence approach was used to monitor subcellular distribution of TNF-α in the ER/Golgi compartment (in permeabilized cells) or at the plasma membrane (in nonpermeabilized cells). BV2 cells treated with LPS exhibited pronounced intracellular TNF-α staining at 3, 6 and 24 h (Figure 4A, panel a). Co-treatment with TFM-C further enhanced intracellular staining of TNF-α, which was validated by flow cytometry and densitometric analysis (Figure 4A panels a and b, and Figure S3). No significant differences were observed in TNF-α staining at the plasma membrane in nonpermeabilized cells between TFM-C/LPS- and LPS-treated cells (Figure S4). This data suggests that the enhanced levels of secreted TNF-α in TFM-C/LPS-treated organotypic cerebellar cultures (Figure 1A) is unlikely to originate from microglial cell sources. Therefore, we analyzed TNF-α production from isolated primary cortical astrocytes, another LPS-inducible natural source of TNF-α in the Central Nervous System (CNS) [37]. As shown in Figure 4B, astrocyte cultures treated with TFM-C alone displayed marginally increased TNF-α release compared with untreated cultures. However, treatment with LPS/TFM-C induced a 2-fold increase in TNF-α secretion compared with the cultures stimulated with LPS only. This result demonstrates that resident astrocytes in the cerebellar organotypic cultures rather than microglia may constitute the source of TNF-α by TFM-C (Figure 1A).

TFM-C suppresses EAE

Previously we demonstrated that celecoxib inhibited EAE in COX-2-deficient mice [16], associated with reduced MOG-specific Th1 cytokines. Thus, TFM-C treatment might be inferred to exert an effect on autoreactive T cells by suppressing production of these cytokines. We examined the effect of TFM-C on EAE induced by immunization with MOG derived peptide, MOG35-55, in which disease development largely depends on encephalitogenic T cells. The administration of TFM-C reduced the severity of EAE when compared with the control group (Figure 5). The incidence of disease in the control group was 93.8% and TFM-C reduced the incidence to 57.1%. The average day of onset was 15.2±3.1 in control group and 16.4 ±2.5 in the TFM-C-treated group. This result indicates that TFM-C limits the severity of disease showing similar effects to celecoxib [16].

TFM-C suppresses IFN-γ and IL-17 production from MOG-reactive T cells

We next examined the effect of TFM-C on MOG35-55-specific T cell responses by *ex vivo* re-challenge with MOG35-55 peptide 10 days after immunization. The proliferative response to MOG35-55 was slightly reduced in celecoxib-treated mice (Figure 6A). TFM-C exhibited a stronger inhibitory effect on MOG35-55-reactive T cell proliferation, even though the overall effect of TFM-C on proliferation was also

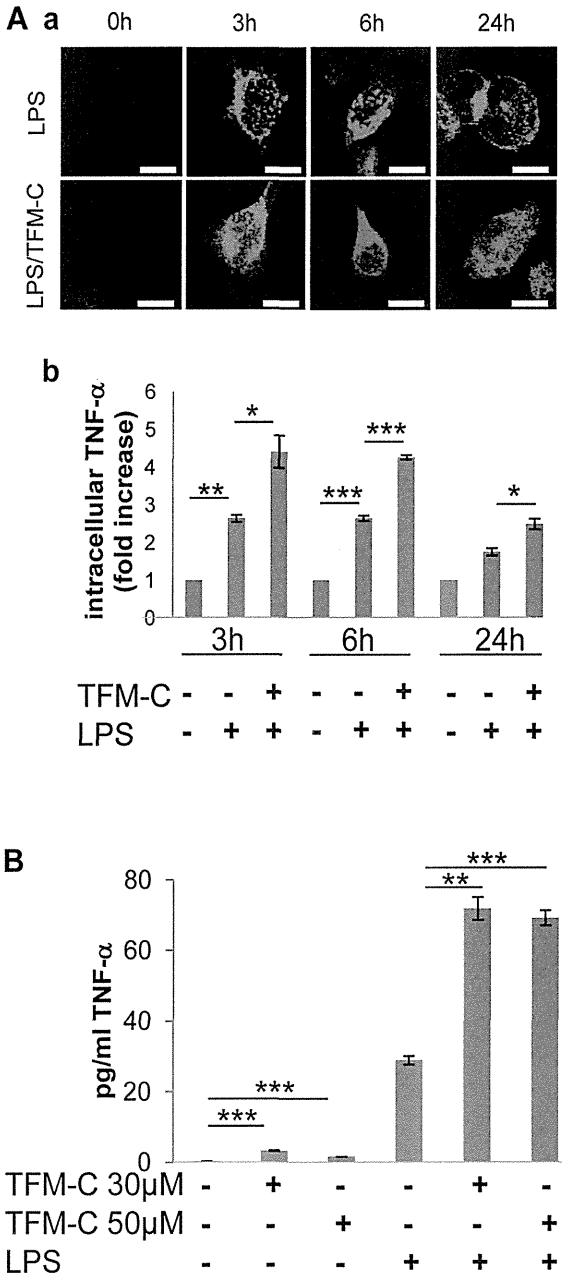

Figure 4. Intracellular localization of TNF-α in BV2 cell line and TNF-α secretion in primary astrocytes. A) BV2 cells were treated with TFM-C (50μM) for 2h and stimulated with LPS (1μg/ml) for 3, 6 and 24h in presence or absence of TFM-C. Panel a) Staining for TNF-α in permeabilized cells. Scale bar 5μm. Panel b) Intracellular localization of TNF-α by flow cytometry. Results are expressed as fold increase compared to the control at the same time point. B) TNF-α release in astrocyte cultures. Astrocytes were treated with TMF-C (30 or 50μM) for 24h or pre-treated with TMF-C for 2h and then stimulated with LPS (1μg/ml) in presence or absence of TFM-C for 24h and then analyzed by ELISA. Error bars indicate the standard deviation. *P<0.05, **P<0.01, ***P<0.001 by ANOVA test.

doi: 10.1371/journal.pone.0083119.g004

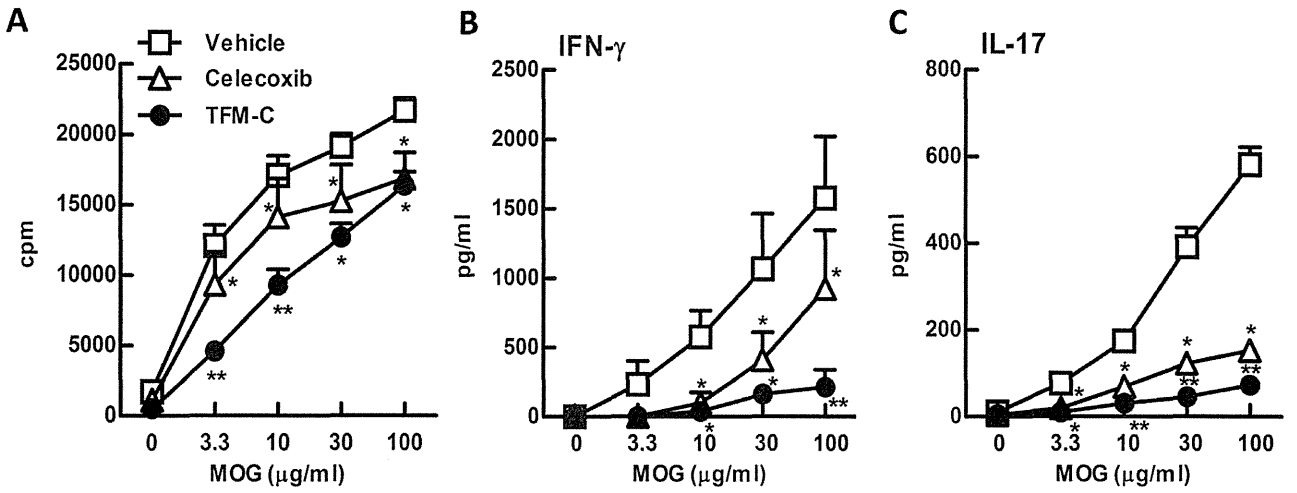

Figure 6. MOG35-55 specific T-cell responses in mice treated with TFM-C. A) Popliteal and inguinal lymph node cells from TFM-C-, celecoxib-treated or control mice were incubated in the presence of MOG35-55 for 48h. Proliferative responses were determined by the uptake of [^{3}H] thymidine. B and C). The levels of IFN-γ and IL-17 in culture supernatants were measured by ELISA. The data shown are from a single experiment representative of three similar experiments. Error bars represent + SEM of 3 mice per group. *P<0.05 compared with control group, **P<0.05 compared with both control and celecoxib-treated groups.

doi: 10.1371/journal.pone.0083119.g006

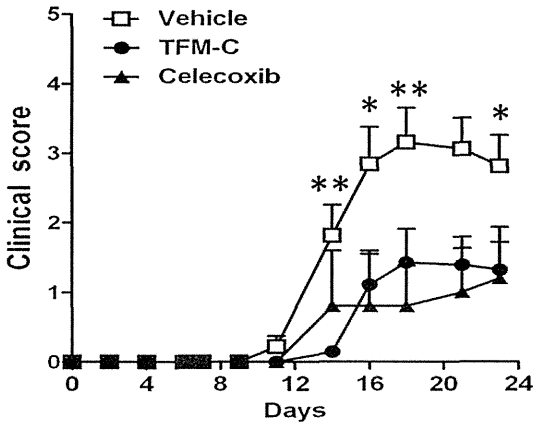

Figure 5. The effect of TFM-C on EAE. Clinical EAE scores of female B6 mice following immunization with MOG35-55. The mice were injected i.p. with 10 μg/kg TFM-C (closed circles), celecoxib (closed triangles) or vehicle (open squares) every other day starting on the day of immunization. *P<0.05 TFM-C-treated versus vehicle-treated group. Results shown are the mean + SEM of 14-16 mice per group in TFM-C- or vehicle-treated groups and of 5 mice in the celecoxib-treated group. The data shown are pooled data from three similar experiments.

doi: 10.1371/journal.pone.0083119.g005

limited (Figure 6A). Compared to control cells, lymph node cells from MOG35-55-primed TFM-C-treated mice produced significantly lower levels of IFN-γ; this was also true for lymph node cells from celecoxib-treated mice albeit to lesser degree (Figure 6B). Furthermore, the level of IL-17 was also significantly reduced in both TFM-C and celecoxib-treated mice compared to that in control mice (Figure 6C). The level of IL-4 was below detection limits (

< 5 pg/ml) (data not shown). These results indicate that TFM-C suppresses MOG35-55-specific T cell proliferation and the production of IL-17 and IFN-γ, and that the suppressive effects of TFM-C on MOG35-55-specific T cell responses are stronger than those of celecoxib.

TFM-C inhibits the production of IL-23 and inflammatory cytokines by dendritic cells

To assess the effect of TFM-C on natural production of IL-12/IL-23, we stimulated Bone Marrow-derived Dendritic Cells (BMDCs) with LPS with or without TFM-C or celecoxib, and measured IL-12 and IL-23 in the culture supernatants. As shown in Figure 7A, IL-23 production was significantly suppressed in the presence of TFM-C. IL-23 suppression was also observed for BMDCs in the presence of celecoxib although the difference did not reach statistical significance. In contrast, neither compound inhibited IL-12 production. To examine the effect on the production of inflammatory cytokines, we stimulated BMDCs with heat-killed *Mtb*, a potent IL-1 stimulator, with or without TFM-C or celecoxib. As shown in Figure 7B, IL-1β, IL-6 and TNF-α production were inhibited in the presence of TFM-C or celecoxib. These results indicate that TFM-C inhibits the production of IL-23 and inflammatory cytokines by BMDCs.

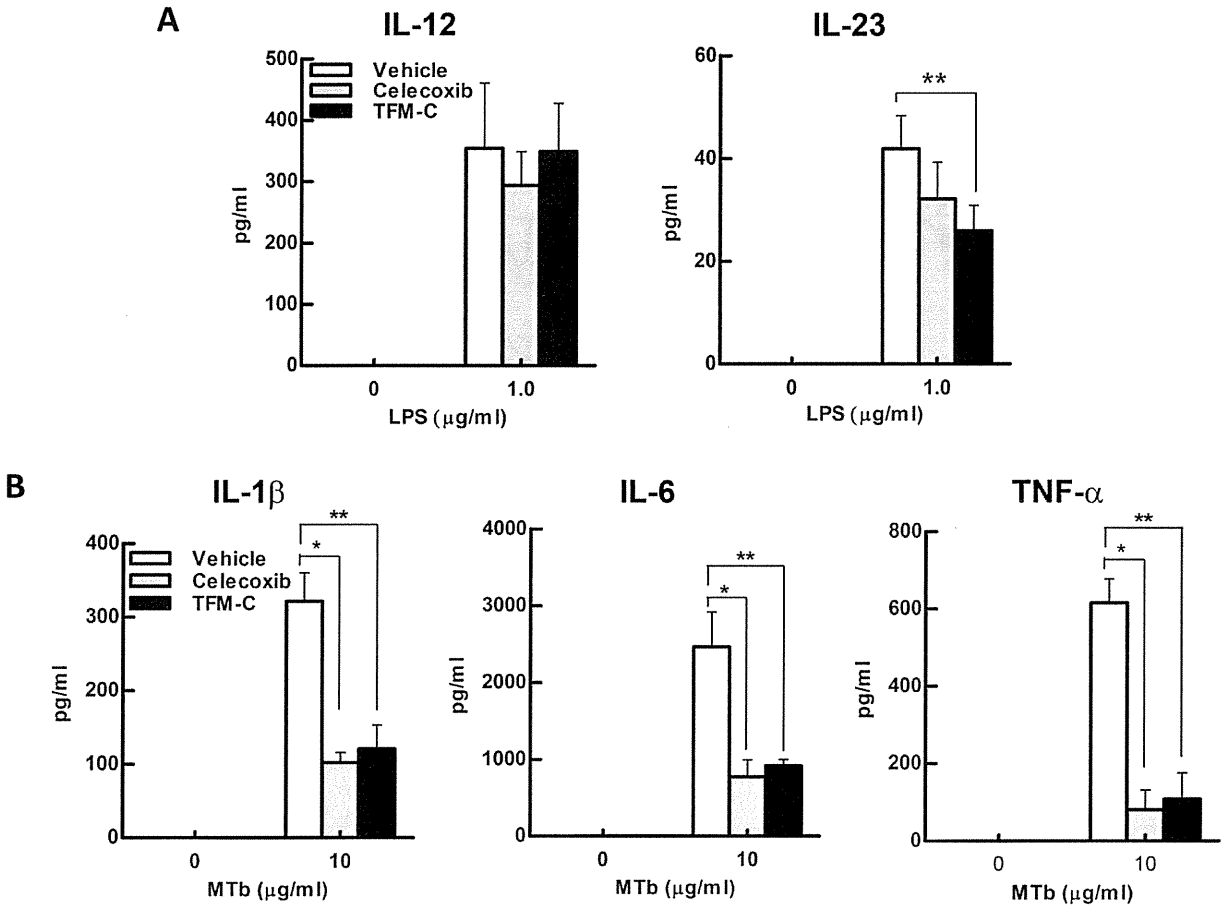

Figure 7. The effect of TFM-C on cytokine production from BMDCs. BMDCs were incubated in TFM-C, celecoxib or vehicle for 16h and subsequently stimulated with LPS (0.1μg/ml) (A) or heat killed H37Ra Mtb (10μg/ml) (B) in the presence of TFM-C, celecoxib or vehicle. Cytokines were detected by ELISA. IL-12, IL-1β or IL-6 were measured 24h after stimulation. IL-23 and TNF-α were measured 6h after stimulation. The data shown are pooled from two similar experiments. Error bars represent + SEM. *P<0.05 control versus TFM-C celecoxib-treated group, **P<0.05 control versus TFM-C -treated group.

doi: 10.1371/journal.pone.0083119.g007

Discussion

In this study, we have tested a non-coxib analogue of celecoxib, TFM-C, both in a model of neuroinflammation consisting of organotypic cultures challenged with LPS [32] and in EAE. The former model recapitulates several events that occur during brain inflammation, including microglia activation followed by cytokine release and oxidative stress, demyelination and axonal damage and permits to study the effect and the mechanism of new treatments for neuroinflammatory disorders [31,32]. Of note, TFM-C significantly decreased axonal damage and oxidative stress in organotypic cultures associated with suppression of IL-1β, IL-12 and IL-17 secretion but enhanced that of TNF-α and RANTES. Similarly to celecoxib in EAE, TFM-C reduced infiltration in CNS, demyelination and production of IFN-γ and IL-17. Further analysis showed that astrocytes cultures treated with TFM-C increased TNF-α release. Moreover, we observed a 2-fold increase in the TNF-α secretion when the astrocytes were co-treated with LPS/TFM-C for 24 hours compared with the cultures stimulated with LPS only. In contrast, in the BV2 microglia cell line, TFM-C suppressed secreted TNF-α protein levels. An explanation for these opposite effects should be sought in the differential response of astrocytes and microglia to modulation of intracellular calcium homoeostasis through selectively inhibiting ER Ca^{2+}-ATPases by celecoxib or TFM-C [5,38]. Astrocytes possess an intracellular Ca^{2+}-dependent excitability leading to glutamate release [39-44]. For example, A23187, a Ca^{2+}-dependent ER stressor, induces elevation of calcium levels, thus increasing glutamate release [45]. In addition, stimulation of astrocytes by glutamate or ATP induces a glutamatergic response accompanied by TNF-α release [46]. However, ionomycin, another Ca^{2+}-dependent ER stressor, does not induce cytokine release in microglia, indicating that in microglia Ca^{2+} perturbation is not sufficient to induce cytokines secretion [47]. These data suggest that the resident astrocytes

and microglia in our cerebellar organotypic cultures respond differentially to Ca^{2+} perturbation by TFM-C in terms of TNF-α secretion.

We also observed a significant increase of RANTES levels in organotypic cultures treated with TFM-C. RANTES is a chemokine that promotes the recruitment and activation of inflammatory cells such as monocytes, lymphocytes, mast cells and eosinophils [48-51]. RANTES also attracts memory T cells, promoting the formation of mononuclear infiltrates characteristic of MS [49,52]. Moreover, it has been described that astrocytes can generate RANTES after stimulation with TNF-α, IL-1β and IFN-γ. Actually, RANTES can be induced only by TNF-α alone in rat primary astrocytes [53].

The role of TNF-α in the pathogenesis of inflammatory demyelinating disease of the central nervous system has been demonstrated in rodents [54] and in humans [55-57]. Transgenic mice that constitutively express TNF-α in the CNS can trigger the development of a chronic inflammatory demyelinating disease [58]. TNF-α is synthesized as a transmembrane precursor protein (tmTNF) and its cytoplasmic tail is cleaved by the TNF-α-converting enzyme (TACE) to release a soluble TNF-α (sTNF). These two forms of TNF-α interact with the receptors, tumor necrosis factor 1 (TNFR1) and 2 (TNFR2). TNFR1 is expressed in all cell types and is preferentially bound by sTNF whereas TNFR2 is expressed by endothelial cells and immune cells and especially bound by tmTNF [59]. The activation of TNFR1 can induce either activation of NFκB or apoptosis via caspase 8 and 3 [60]. The binding to TNFR2 induces proinflammatory and survival signaling pathways [61]. Comparison of TNFR1 and TNFR1/TNFR2 knockout and wild-type mice, shows that EAE symptoms were milder or absent in the knockout animals. In contrast, in TNFR2-deficient mice the symptoms were enhanced and associated with high inflammation and demyelination [62,63]. Remyelinated function was conferred to TNFR2 whereas demyelination to TNFR1 [64]. Recently, we have shown that demyelination was significantly attenuated in cerebellar cultures challenged with LPS pretreated with Fc-TNFR1 recombinant protein [32]. In particular, we found that myelin damage and oligodendrocyte loss were promoted by pro-inflammatory cytokines such as TNF-α. Probably, the observation that the TFM-C treatment had no effect on demyelination in organotypic culture model could be explained by increased astrocytic TNF-α, that in turn induces TNFR1 activation. Moreover, immune cells expressing TNFR2 are lacking in organotypic cultures. In contrast, in the same model TFM-C exerts beneficial effects restoring oxidative stress and axonal damage induced by LPS.

In the EAE model, although the treatment with TFM-C failed to completely inhibit the development of EAE, TFM-C significantly reduced the severity of the disease decreasing the incidence from 93.8% to 57.1%. Moreover, TFM-C suppressed the production of IL-23 and inflammatory cytokines, IL-1β, IL-6 and TNF-α from dendritic cells and this suppressive effect was strong enough to decrease the subsequent production of IL-17 and IFN-γ from lymph node cells upon stimulation with MOG. The differential effects observed on IL-23 inhibition by celecoxib vs TFM-C suggest a beneficial effect of the latter via inhibition of the Th17 responses. In addition to the suppression of IL-23, blockage of IL-6 and IL-1β, two cytokines that affect development of Th17 cells, would also contribute to the suppression of IL-17 [65,66]. TNF-α, IL-1β and IL-6 can increase the permeability of the blood-brain barrier (BBB) [67]. IL-6 induces leukocyte chemoattraction to the endothelium, as well as lymphocyte activation. IL-6 is found in high concentrations in active MS lesions [68,69]. In EAE, IL-6 induction is found in the spinal cord [70]. The detrimental role of IL-6 in this model, associated with BBB permeability, is evidenced in IL-6-deficient mice that are resistant to the pathophysiological alterations [71]; on the other hand, mice overexpressing astrocytic IL-6 showed indeed breakdown of the BBB [72]. Moreover, the inhibition of IL-6 in BMDCs and macrophages [17] treated with TFM-C might suggest that the beneficial effect of TFM-C in EAE can depend on its ability to reduce BBB permeability.

The different effect of TFM-C observed in CNS-derived cells versus lymph node-derived cells may reside in incomplete penetration of TFM-C into CNS. In the *in vivo* system, TFM-C may exert a beneficial effect on peripheral cells, reducing proliferation and pro-inflammatory cytokine secretion, thus ameliorating disease severity. In contrast, when CNS cells are exposed directly to TFM-C, such as in the organotypic, astrocyte or microglia cultures, these cells may respond to Ca^{2+} perturbation differentially by either increasing or decreasing pro-inflammatory cytokine secretion. However, it remains to be determined whether TFM-C penetrates into the intact CNS following i.p. injection. If not, the main cellular mediators of its cytokine-modulating effects are likely to be the peripheral immune cells. This could explain why TFM-C failed to inhibit completely the development of EAE. In summary, we have described a new drug with potential beneficial effects for MS. The therapeutic niche covered by TFM-C may include beneficial effects in both innate and adaptive immunity, which is incompletely covered by current therapies [73]. In this sense, the therapy can be defined as acting in the interface between immunomodulation and neuroprotection. Thus, design of further non-coxib celecoxib analogues with improved activity profiles may be warranted.

Supporting Information

Figure S1. Effect of TFM-C on MHCII protein expression. Organotypic cultures were stimulated with LPS for 24h or pre-treated with TFM-C (50μM) for 2h and then stimulated with LPS/TFM-C for 24h. Immunofuorescence for Iba1 (red) and MHCII (green) was performed. White boxes show higher magnifications of merged images. Scale bar 50μm.
(TIF)

Figure S2. Effect of TFM-C on expression of genes belonging to Unfolded Protein Response (U), Ubiquitination (Ub) and Autophagy (A) pathways in HEK-293 cells and BV2 cells. A) HEK-293 cells were treated with TFM-C (50μM) for 12h and U, Ub and A PCR arrays were performed. The genes represented in the table are those with a fold increase higher than 2.5 compared with control samples

and are ranked according to expression level (high to low). B) HEK-293 cells were treated with TFM-C (50μM) for different times and RT-QPCR was performed. Selected genes (*PARK2, FBXO4, RAB24, MAP1LCB3, HERP* and *ARMET*) were validated in three independent experiments. The levels of mRNA are shown as $2^{-\Delta\Delta Ct}$ compared with the level of baseline condition (-) and normalized with the housekeeping geneGlyceraldehyde 3-phosphate dehydrogenase. Asterisks indicate significant differences at *P<0.05 by Student's test. C) 20μg of total protein were loaded for PARK2, FBXO4, RAB24, MAP1LCB3, HERP, ARMET and tubulin Western blot analysis D) BV2 cells were pre-treated with TFM-C (30 or 50μM) for 2h, then stimulated with LPS for different times and 10μg of total protein were loaded for Western blot analysis. Results were expressed as arbitrary units compared to the control at same time point. All values represent the averages of three independent experiments. Error bars indicate the standard error. *P<0.05, **P<0.01, ***P<0.001 by ANOVA test.
(TIF)

Figure S3. Quantification of intracellular TNF-α in BV2 cell line. The cells were treated as described in Figure 5 and the fluorescence intensity was analyzed via densitometry using a fluorescence microscope by calculating mean grey value (pixel intensity) normalized by fixed area (ROI=Region Of Interest; Image J Software). For each condition ten cells/field were analyzed for a total of 4 fields and 40 cells. Error bars indicate the standard error.
(TIF)

Figure S4. Quantification of TNF-α in plasma membrane of BV2 cell line. BV2 cells were treated with TFM-C (50μM) for 2h and stimulated with LPS (1μg/ml) for 3, 6 and 24h in presence or absence of TFM-C. The cells were fixed with PFA and stained for TNF-α. A) Fluorescence intensity was analyzed by densitometry calculating mean pixel intensity normalized by ROI fixed area (Image J Software). For each condition ten cells/field were analyzed for a total of 4 fields and 40 cells. Error bars indicate the standard error. B) Staining for TNF-α in non-permeabilized cells. Scale bar 5μm.
(TIF)

Figure S5. Normalization of protein expression. BV2 cells were treated with TFM-C (50μM) for different times and 10μg of total protein were loaded in Stain-free Precast Gels and then transferred to nitrocellulose membrane. A) Total protein was visualized by UV excitation. B) Tubulin protein expression analyzed by Western blot. C) Quantification of HERP band intensity normalized with total protein loaded. D) Quantification of HERP band intensity normalized with Tubulin protein. The values represent the averages of three independent experiments. Significant differences at *P<0.05 and **P<0.01 compared with control (0h) by Student's test.
(TIF)

Acknowledgements

Technical and human support provided by SGIker (UPV/EHU, MICINN, GV/EJ, ESF) is gratefully acknowledged for cytometry and confocal microscopy.

Author Contributions

Performed the experiments: AdP AC AW. Analyzed the data: AdP AC IA TY PV SM KV. Contributed reagents/materials/ analysis tools: KV PV SM TY. Wrote the manuscript: AdP AC SM KV. Carried out the microscopy, molecular studies, organotypic cultures, EAE model and performed the statistical analysis: AdP AC. Performed astrocytes cultures: AW. Participated in the design and interpretation of the study: AdP AC IA PV SM TY KV. Read and approved the final manuscript: AdP AC IA AW PV SM TY KV.

References

1. Shi S, Klotz U (2008) Clinical use and pharmacological properties of selective COX-2 inhibitors. Eur J Clin Pharmacol 64: 233-252. doi: 10.1007/s00228-007-0400-7. PubMed: 17999057.
2. DeWitt DL (1999) Cox-2-selective inhibitors: the new super aspirins. Mol Pharmacol 55: 625-631. PubMed: 10101019.
3. Grösch S, Tegeder I, Niederberger E, Bräutigam L, Geisslinger G (2001) COX-2 independent induction of cell cycle arrest and apoptosis in colon cancer cells by the selective COX-2 inhibitor celecoxib. FASEB J 15: 2742-2744. PubMed: 11606477.
4. Kulp SK, Yang YT, Hung CC, Chen KF, Lai JP et al. (2004) 3-phosphoinositide-dependent protein kinase-1/Akt signaling represents a major cyclooxygenase-2-independent target for celecoxib in prostate cancer cells. Cancer Res 64: 1444-1451. doi: 10.1158/0008-5472.CAN-03-2396. PubMed: 14973075.
5. Alloza I, Baxter A, Chen Q, Matthiesen R, Vandenbroeck K (2006) Celecoxib inhibits interleukin-12 alphabeta and beta2 folding and secretion by a novel COX2-independent mechanism involving chaperones of the endoplasmic reticulum. Mol Pharmacol 69: 1579-1587. doi:10.1124/mol.105.020669. PubMed: 16467190.
6. McLaughlin M, Alloza I, Quoc HP, Scott CJ, Hirabayashi Y et al. (2010) Inhibition of secretion of interleukin (IL)-12/23 family cytokines by 4-trifluoromethyl-celecoxib is coupled to degradation via the endoplasmic reticulum stress protein HERP. J Biol Chem 285: 6960-6969. doi: 10.1074/jbc.M109.056614. PubMed: 20054003.
7. Vandenbroeck K, Alloza I, Brehmer D, Billiau A, Proost P et al. (2002) The conserved helix C region in the superfamily of interferon-gamma / interleukin-10-related cytokines corresponds to a high-affinity binding site for the HSP70 chaperone DnaK. J Biol Chem277: 25668-25676. doi:10.1074/jbc.M202984200. PubMed: 11970958.
8. Vandenbroeck K, Martens E, Alloza I (2006) Multi-chaperone complexes regulate the folding of interferon-gamma in the endoplasmic reticulum. Cytokine 33: 264-273. doi:10.1016/j.cyto.2006.02.004. PubMed: 16574426.
9. McLaughlin M, Vandenbroeck K (2011) The endoplasmic reticulum protein folding factory and its chaperones: new targets for drug discovery? Br J Pharmacol 162: 328-345. doi:10.1111/j.1476-5381.2010.01064.x. PubMed: 20942857.
10. Johnson AJ, Hsu AL, Lin HP, Song X, Chen CS (2002) The cyclo-oxygenase-2 inhibitor celecoxib perturbs intracellular calcium by inhibiting endoplasmic reticulum Ca2+-ATPases: a plausible link with its anti-tumour effect and cardiovascular risks. Biochem J 366: 831-837. PubMed: 12076251.
11. Kardosh A, Golden EB, Pyrko P, Uddin J, Hofman FM et al. (2008) Aggravated endoplasmic reticulum stress as a basis for enhanced glioblastoma cell killing by bortezomib in combination with celecoxib or its non-coxib analogue, 2,5-dimethyl-celecoxib. Cancer Res, 68: 843-851. doi:10.1158/0008-5472.CAN-07-5555. PubMed: 18245486.
12. Okada T, Yoshida H, Akazawa R, Negishi M, Mori K (2002) Distinct roles of activating transcription factor 6 (ATF6) and double-stranded RNA-activated protein kinase-like endoplasmic reticulum kinase (PERK) in transcription during the mammalian unfolded protein

response. Biochem J 366: 585–594. doi:10.1042/BJ20020391. PubMed: 12014989.
13. Oyadomari S, Mori M (2004) Roles of CHOP/GADD153 in endoplasmic reticulum stress. Cell Death Differ 11: 381–389. doi:10.1038/sj.cdd.4401373. PubMed: 14685163.
14. Ni J, Shu YY, Zhu YN, Fu YF, Tang W et al. (2007) COX-2 inhibitors ameliorate experimental autoimmune encephalomyelitis through modulating IFN-gamma and IL-10 production by inhibiting T-bet expression. J Neuroimmunol 186: 94-103. doi:10.1016/j.jneuroim.2007.03.012. PubMed: 17442406.
15. Reder AT, Thapar M, Sapugay AM, Jensen MA (1994) Prostaglandins and inhibitors of arachidonate metabolism suppress experimental allergic encephalomyelitis. J Neuroimmunol 54: 117-127. doi:10.1016/0165-5728(94)90238-0. PubMed: 7523442.
16. Miyamoto K, Miyake S, Mizuno M, Oka N, Kusunoki S et al. (2006) Selective COX-2-inhibitor celecoxib prevents experimental autoimmune encephalomyelitis through COX-2-independent pathway. Brain 129: 1984-1992. doi:10.1093/brain/awl170. PubMed: 16835249.
17. Chiba A, Mizuno M, Tomi C, Tajima R, Alloza I, et al. (2012) A 4-trifluoromethyl analogue of celecoxib inhibits arthritis by suppressing innate immune cell activation. Arthritis Res Ther 14: R9.
18. Trelle S, Reichenbach S, Wandel S, Hildebrand P, Tschannen B et al. (2011) Cardiovascular safety of non-steroidal anti-inflammatory drugs: network meta-analysis. BMJ 342: c7086. doi:10.1136/bmj.c7086. PubMed: 21224324.
19. Ray WA, Varas-Lorenzo C, Chung CP, Castellsague J, Murray KT et al. (2009) Cardiovascular risks of nonsteroidal antiinflammatory drugs in patients after hospitalization for serious coronary heart disease. Circ Cardiovasc Qual Outcomes 2: 155-163. doi:10.1161/CIRCOUTCOMES.108.805689. PubMed: 20031832.
20. Solomon SD, Wittes J, Finn PV, Fowler R, Viner J et al. (2008) Cardiovascular risk of celecoxib in 6 randomized placebo-controlled trials: the cross trial safety analysis. Circulation 117: 2104-2113. doi:10.1161/CIRCULATIONAHA.108.764530. PubMed: 18378608.
21. Feng GS, Ma JL, Wong BC, Zhang L, Liu WD, et al. (2008) Celecoxib-related gastroduodenal ulcer and cardiovascular events in a randomized trial for gastric cancer prevention. World J Gastroenterol 14: 4535-4539.
22. Haag MDM, Bos MJ, Hofman A, Koudstaal PJ, Breteler MMB et al. (2008) Cyclooxygenase selectivity of nonsteroidal anti-inflammatory drugs and risk of stroke. Arch Intern Med 168: 1219-1224. doi:10.1001/archinte.168.11.1219. PubMed: 18541831.
23. Grosser T, Fries S, FitzGerald GA (2006) Biological basis for the cardiovascular consequences of COX-2 inhibition: Therapeutic challenges and opportunities. J Clin Invest 116: 4–15. PubMed: 16395396.
24. Pidgeon GP, Tamosiuniene R, Chen G, Leonard I, Belton O et al. (2004) Intravascular thrombosis after hypoxia-induced pulmonary hypertension: regulation by cyclooxygenase-2. Circulation 110: 2701–2707. doi:10.1161/01.CIR.0000145613.01188.0B. PubMed: 15492320.
25. Buerkle MA, Lehrer S, Sohn H-Y, Conzen P, Pohl U et al. (2004) Selective inhibition of cyclooxygenase-2 enhances platelet adhesion in hámster arterioles in vivo. Circulation 110: 2053–2059. doi:10.1161/01.CIR.0000143234.51796.A9. PubMed: 15451781.
26. Stoppini L, Buchs PA, Muller D (1991) A simple method for organotypic cultures of nervous tissue. J Neurosci Methods 37: 173-182. doi:10.1016/0165-0270(91)90128-M. PubMed: 1715499.
27. Dusart I, Airaksinen MS, Sotelo C (1997) Purkinje cell survival and axonal regeneration are age dependent: an in vitro study. J Neurosci 17: 3710-3726. PubMed: 9133392.
28. Blasi E, Barluzzi R, Bocchini V, Mazzolla R, Bistoni F (1990) Immortalization of murine microglial cells by a v-raf/v-myc carrying retrovirus. J Neuroimmunol 27: 229-237. doi:10.1016/0165-5728(90)90073-V. PubMed: 2110186.
29. McCarthy KD, de Vellis J (1980) Preparation of separate astroglial and oligodendroglial cell cultures from rat cerebral tissue. J Cell Biol 85: 890-902. doi:10.1083/jcb.85.3.890. PubMed: 6248568.
30. Fan LW, Tien LT, Mitchell HJ, Rhodes PG, Cai Z (2008) Alpha-phenyl-n-tert-butyl-nitrone ameliorates hippocampal injury and improves learning and memory in juvenile rats following neonatal exposure to lipopolysaccharide. Eur J Neurosci 27: 1475-1484.
31. Kim JY, Shen S, Dietz K, He Y, Howell O et al. (2010) HDAC1 nuclear export induced by pathological conditions is essential for the onset of axonal damage. Nat Neurosci 13: 180-189. doi:10.1038/nn.2471. PubMed: 20037577.
32. Di Penta A, Moreno B, Reix S, Fernandez-Diez B, Villanueva M et al. (2013) Oxidative stress and proinflammatory cytokines contribute to demyelination and axonal damage in a cerebellar culture model of neuroinflammation. PLOS_ONE 8: e54722. doi:10.1371/journal.pone.0054722.
33. Sherwin C, Fern R (2005) Acute lipopolysaccharide-mediated injury in neonatal white matter glia: role of TNF-alpha, IL-1beta, and calcium. J Immunol 175: 155-161. PubMed: 15972642.
34. Coleman M (2005) Axon degeneration mechanisms: commonality amid diversity. Nat Rev Neurosci 6: 889-898. doi:10.1038/nrn1788. PubMed: 16224497.
35. Wheeler MC, Rizzi M, Sasik R, Almanza G, Hardiman G, et al. (2008) KDEL-retained antigen in B lymphocytes induces a proinflammatory response: a possible role for endoplasmic reticulum stress in adaptive T cell immunity. J Immunol 181: 256-264.
36. Ron D, Habener JF (1992) CHOP, a novel developmentally regulated nuclear protein that dimerizes with transcription factors C/EBP and LAP and functions as a dominant-negative inhibitor of gene transcription. Genes Dev 6: 439–453. doi:10.1101/gad.6.3.439. PubMed: 1547942.
37. Chung IY, Benveniste EN (1990) Tumor necrosis factor-alpha production by astrocytes. Induction by lipopolysaccharide, IFN-gamma, and IL-1 beta. J Immunol 144: 2999-3007.
38. Johnson AJ, Hsu AL, Lin HP, Song X, Chen CS (2002) The cyclo-oxygenase-2 inhibitor celecoxib perturbs intracellular calcium by inhibiting endoplasmic reticulum Ca2+-ATPases: a plausible link with its anti-tumour effect and cardiovascular risks. Biochem J 366: 831-837. PubMed: 12076251.
39. Cornell-Bell AH, Finkbeiner SM, Cooper MS, Smith SJ (1990) Glutamate induces calcium waves in cultured astrocytes: long-range glial signaling. Science 247: 470-473.
40. Charles AC, Merrill JE, Dirksen ER, Sanderson MJ (1991) Intercellular signaling in glial cells: calcium waves and oscillations in response to mechanical stimulation and glutamate. Neuron 6: 983-992. doi:10.1016/0896-6273(91)90238-U. PubMed: 1675864.
41. Parpura V, Basarsky TA, Liu F, Jeftinija K, Jeftinija S et al. (1994) Glutamate-mediated astrocyte-neuron signalling. Nature 369: 744 – 747. doi:10.1038/369744a0. PubMed: 7911978.
42. Pasti L, Volterra A, Pozzan T, Carmignoto G (1997) Intracellular calcium oscillations in astrocytes: a highly plastic, bidirectional form of communication between neurons and astrocytes in situ. J Neurosci 17: 7817–7830. PubMed: 9315902.
43. Newman EA, Zahs KR (1997) Calcium waves in retinal glial cells. Science 275: 844–857. doi:10.1126/science.275.5301.844. PubMed: 9012354.
44. Bezzi P, Carmignoto G, Pasti L, Vesce S, Rossi D et al. (1998) Prostaglandins stimulate calciumdependent glutamate release in astrocytes. Nature 391: 281–285. doi:10.1038/34651. PubMed: 9440691.
45. Innocenti B, Parpura V, Haydon PG (2000) Imaging extracellular waves of glutamate during calcium signaling in cultured astrocytes. J Neurosci 20: 1800-1808. PubMed: 10684881.
46. Bezzi P, Domercq M, Brambilla L, Galli R, Schols D et al. (2001) CXCR4-activated astrocyte glutamate release via TNFalpha: amplification by microglia triggers neurotoxicity. Nat Neurosci 4: 702-710. doi:10.1038/89490. PubMed: 11426226.
47. Hoffmann A, Kann O, Ohlemeyer C, Hanisch UK, Kettenmann H (2003) Elevation of basal intracellular calcium as a central element in the activation of brain macrophages (microglia): suppression of receptor-evoked calcium signaling and control of release function. J Neurosci 23: 4410-4419
48. Meurer R, Van Riper G, Feeney W, Cunningham P, Hora D Jr et al. (1993) Formation of eosinophilic and monocytic intradermal inflammatory sites in the dog by injection of human RANTES but not human monocyte chemoattractant protein 1, human macrophage inflammatory protein 1 alpha, or human interleukin 8. J Exp Med 178: 1913-1921. doi:10.1084/jem.178.6.1913. PubMed: 7504053.
49. Schall TJ, Bacon K, Toy KJ, Goeddel DV (1990) Selective attraction of monocytes and T lymphocytes of the memory phenotype by cytokine RANTES. Nature 347: 669-671. doi:10.1038/347669a0. PubMed: 1699135.
50. Conti P, Reale M, Barbacane RC, Letourneau R, Theoharides TC (1998) Intramuscular injection of hrRANTES causes mast cell recruitment and increased transcription of histidine decarboxylase in mice: lack of effects in genetically mast cell-deficient W/WV mice. FASEB J 12: 1693-1700. PubMed: 9837859.
51. Das AM, Ajuebor MN, Flower RJ, Perretti M, McColl SR (1999) Contrasting roles for RANTES and macrophage inflammatory protein-1 alpha (MIP-1 alpha) in a murine model of allergic peritonitis. Clin Exp Immunol 117: 223-229. doi:10.1046/j.1365-2249.1999.00978.x. PubMed: 10444251.
52. Weber C, Weber KS, Klier C, Gu S, Wank R et al. (2001) Specialized roles of the chemokine receptors CCR1 and CCR5 in the recruitment of

monocytes and T(H)1-like/CD45RO(+) T cells. Blood 97: 1144–1146. doi:10.1182/blood.V97.4.1144. PubMed: 11159551.
53. Barnes DA, Huston M, Holmes R, Benveniste EN, Yong VW et al. (1996) Induction of RANTES expression by astrocytes and astrocytoma cell lines. J Neuroimmunol 71: 207-214. doi:10.1016/S0165-5728(96)00154-3. PubMed: 8982121.
54. Selmaj K, Raine CS, Cross AH (1991) Anti-tumor necrosis factor therapy abrogates autoimmune demyelination. Ann Neurol 30: 694–700. doi:10.1002/ana.410300510. PubMed: 1722388.
55. Baker D, Butler D. D, Scallon BJ, O'Neill JK, Turk JL et al. (1994) Control of established experimental allergic encephalomyelitis by inhibition of tumor necrosis factor (TNF) activity within the central nervous system using monoclonal antibodies and TNF receptor-immunoglobulin fusion proteins. Eur J Immunol 24: 2040–2048. doi:10.1002/eji.1830240916. PubMed: 8088324. Available online at: doi:10.1002/eji.1830240916 Available online at: PubMed: 8088324
56. Hofman FM, Hinton DR, Johnson K, Merrill JE (1989) Tumor necrosis factor identified in multiple sclerosis brain. J Exp Med, 170: 607–612. doi:10.1084/jem.170.2.607. PubMed: 2754393.
57. Sharief MK, Hentges R (1991) Association between tumor necrosis factor-alpha and disease progression in patients with multiple sclerosis. N Engl J Med 325: 467–472. doi:10.1056/NEJM199108153250704. PubMed: 1852181.
58. Probert L, Akassoglou K, Pasparakis M, Kontogeorgos G, Kollias G (1995) Spontaneous inflammatory demyelinating disease in transgenic mice showing central nervous system-specific expression of tumor necrosis factor alpha. Proc Natl Acad Sci U S A 92: 11294-11298. doi:10.1073/pnas.92.24.11294. PubMed: 7479982.
59. Grell M, Wajant H, Zimmermann G, Scheurich P (1998) The type 1 receptor (CD120a) is the high-affinity receptor for soluble tumor necrosis factor. Proc Natl Acad Sci U S A 95: 570–575. doi:10.1073/pnas.95.2.570. PubMed: 9435233.
60. Tracey D, Klareskog L, Sasso EH, Salfeld JG, Tak PP (2008) Tumor necrosis factor antagonist mechanisms of action: a comprehensive review. Pharmacol Ther 117: 244–279. doi:10.1016/j.pharmthera.2007.10.001. PubMed: 18155297.
61. Yang L, Lindholm K, Konishi Y, Li R, Shen Y (2002) Target depletion of distinct tumor necrosis factor receptor subtypes reveals hippocampal neuron death and survival through different signal transduction pathways. J Neurosci 22: 3025–3032. PubMed: 11943805.
62. Suvannavejh GC, Lee HO, Padilla J, Dal Canto MC, Barrett TA et al. (2000) Divergent roles for p55 and p75 tumor necrosis factor receptors in the pathogenesis of MOG (35–55)-induced experimental autoimmune encephalomyelitis. Cell Immunol 205: 24–33. doi:10.1006/cimm.2000.1706. PubMed: 11078604.
63. Kassiotis G, Kollias G (2001) Uncoupling the proinflammatory from the immunosuppressive properties of tumor necrosis factor (TNF) at the p55 TNF receptor level: implications for pathogenesis and therapy of autoimmune demyelination. J Exp Med 193: 427–434. doi:10.1084/jem.193.4.427. PubMed: 11181695.
64. Caminero A, Comabella M, Montalban X (2011) Tumor necrosis factor alpha (TNF-α), anti-TNF-α and demyelination revisited: an ongoing story. J Neuroimmunol 234: 1-6. doi:10.1016/j.jneuroim.2011.03.004. PubMed: 21474190.
65. Bettelli E, Carrier Y, Gao W, Korn T, Strom TB et al. (2006) Reciprocal developmental pathways for the generation of pathogenic effector Th17 and regulatory T cells. Nature 441: 235-238. doi:10.1038/nature04753. PubMed: 16648838.
66. Veldhoen M, Hocking RJ, Atkins CH, Locksley RM, Stockinger B (2006) TGFbeta in the context of an inflammatory cytokine milieu supports de novo differentiation ofmIL-17-producin cells. Immunity 24: 179-189. doi:10.1016/j.immuni.2006.01.001. PubMed: 16473830.
67. de Vries HE, Blom-Roosemalen MC, van Oosten M, de Boer AG, van Berkel TJ et al. (1996) The influence of cytokines on the integrity of the blood-brain barrier in vitro. J Neuroimmunol 64: 37-43. doi:10.1016/0165-5728(95)00148-4. PubMed: 8598388.
68. Cannella B, Raine CS (1995) The adhesion molecule and cytokine profile of multiple sclerosis lesions. Ann Neurol 37: 424-435. doi:10.1002/ana.410370404. PubMed: 7536402.
69. Woodroofe MN, Cuzner ML (1993) Cytokine mRNA expression in inflammatory multiple sclerosis lesions: detection by non-radioactive in situ hybridization. Cytokine 5: 583-588. doi:10.1016/S1043-4666(05)80008-0. PubMed: 8186370.
70. Agnello D, Bigini P, Villa P, Mennini T, Cerami A et al. (2002) Erythropoietin exerts an anti-inflammatory effect on the CNS in a model of experimental autoinmune encephalomyelitis. Brain Res 952: 128-134. doi:10.1016/S0006-8993(02)03239-0. PubMed: 12363412.
71. Eugster HP, Frei K, Kopf M, Lassmann H, Fontana A (1998) IL-6-deficient mice resist myelin oligodendrocyte glycoprotein-induced autoimmune encephalomyelitis. Eur J Immunol 28: 2178-2187. doi:10.1002/(SICI)1521-4141(199807)28:07. PubMed: 9692887.
72. Brett FM, Mizisin AP, Powell HC, Campbell IL (1995) Evolution of neuropathologic abnormalities associated with blood-brain barrier breakdown in transgenic mice expressing interleukin-6 in astrocytes. J Neuropathol Exp Neurol 54: 766-775. doi:10.1097/00005072-199511000-00003. PubMed: 7595649.
73. Castro-Borrero W, Graves D, Frohman TC, Bates Flores A, Hardeman P et al. (2012) Current and emerging therapies in multiple sclerosis: a systematic review. Ther Adv Neurol Disord 5: 205-220. doi:10.1177/1756285612450936. PubMed: 22783370.

DNA Research **20**, 241–253, (2013)
Advance Access publication on 9 April 2013
doi:10.1093/dnares/dst006

Robustness of Gut Microbiota of Healthy Adults in Response to Probiotic Intervention Revealed by High-Throughput Pyrosequencing

Seok-Won Kim[1], Wataru Suda[1], Sangwan Kim[1], Kenshiro Oshima[1], Shinji Fukuda[2,3,4], Hiroshi Ohno[3,4], Hidetoshi Morita[5], and Masahira Hattori[1,*]

Center for Omics and Bioinformatics, The Department of Computational Biology, Graduate School of Frontier Sciences, The University of Tokyo, Kashiwanoha 5-1-5, Kashiwa, Chiba 277-8561, Japan[1]; Institute for Advanced Biosciences, Keio University, Mizukami 246-2, Kakuganji, Tsuruoka City, Yamagata 997-0052, Japan[2]; Laboratory for Epithelial Immunobiology, RIKEN Research Center for Allergy and Immunology, Yokohama, Japan[3]; Graduate School of Nanobioscience, Yokohama City University, Yokohama 230-0045, Japan[4] and School of Veterinary Medicine, Azabu University, Fuchinobe 1-17-71, Chuo-ku, Sagamihara, Kanagawa 252-5201, Japan[5]

*To whom correspondence should be addressed. Tel. +81 4-7136-4070. Fax. +81 4-7136-4084.
Email: hattori@k.u-tokyo.ac.jp

Edited by Dr Katsumi Isono
(Received 12 December 2012; accepted 16 February 2013)

Abstract

Probiotics are live microorganisms that potentially confer beneficial outcomes to host by modulating gut microbiota in the intestine. The aim of this study was to comprehensively investigate effects of probiotics on human intestinal microbiota using 454 pyrosequencing of bacterial 16S ribosomal RNA genes with an improved quantitative accuracy for evaluation of the bacterial composition. We obtained 158 faecal samples from 18 healthy adult Japanese who were subjected to intervention with 6 commercially available probiotics containing either *Bifidobacterium* or *Lactobacillus* strains. We then analysed and compared bacterial composition of the faecal samples collected before, during, and after probiotic intervention by Operational taxonomic units (OTUs) and UniFrac distances. The results showed no significant changes in the overall structure of gut microbiota in the samples with and without probiotic administration regardless of groups and types of the probiotics used. We noticed that 32 OTUs (2.7% of all analysed OTUs) assigned to the indigenous species showed a significant increase or decrease of ≥10-fold or a quantity difference in >150 reads on probiotic administration. Such OTUs were found to be individual specific and tend to be unevenly distributed in the subjects. These data, thus, suggest robustness of the gut microbiota composition in healthy adults on probiotic administration.

Key words: probiotics; gut microbiota; 16S ribosomal RNA gene; pyrosequencing

1. Introduction

Probiotics are defined as live bacterial strains conferring various benefits to the consumer by modulating the intestinal ecosystem, thereby potentially promoting host health and improving host disease risk.[1–11] Various probiotic strains have been industrially developed and marketed as a variety of products and applications such as fermented foods and supplements, including yogurt[12–15] Most probiotics taxonomically belong to two genera, *Bifidobacterium* and *Lactobacillus*, that originate from various environments, including the human intestine, and both species are generally regarded as safe.[16–18]

The interaction between administrated probiotics and indigenous microbiota is one of the most attractive and important research areas, particularly because gut microbiota have been shown to be profoundly